Techno-economic evaluation of energy markets for demand response and congestion management in future decentralized energy systems

Pedro Iván Leal Jáuregui

TU Delft

TECHNO-ECONOMIC EVALUATION OF ENERGY MARKETS FOR DEMAND RESPONSE AND CONGESTION MANAGEMENT IN FUTURE DECENTRALIZED ENERGY SYSTEMS

A thesis submitted to the Delft University of Technology
to obtain the degree of

Master of Science in Sustainable Energy Technology

by

Pedro Iván Leal Jáuregui

to be defended publicly on the 28$^{\text{th}}$ of February, 2022

The work in this thesis was made in the:

Delft University of Technology

Student number:	5006341	
Thesis committee:	Prof. dr. ir. P. Bauer,	TU Delft, chair
	Dr. ir. G.R. Chandra Mouli,	TU Delft, supervisor
	Dr. ir. Aleksandra Lekic	TU Delft
Advisor:	ir. Wiljan Vermeer	TU Delft

ABSTRACT

In the context of the energy transition, the energy sector is experiencing a paradigm shift towards electrification in a decentralized model, where renewable energy sources are becoming the protagonists. However, such shift comes with several challenges. In particular for this thesis, the intermittency of renewable energy sources coupled with increased load demand and generation from small scale prosumers is expected to increase grid congestion at a distribution level.

The main purpose of this thesis is to investigate and evaluate the techno-economic feasibility of novel market mechanisms that incentivize demand response from prosumers for congestion management. The focus of this work is on market-based mechanisms that use economic signals to stir prosumers' demand response. The mechanisms investigated are: 1) hard constraint that physically limits prosumers, 2) capacity subscription, 3) peak tariff, and 4) dynamic tariff; these are capacity mechanisms that limit the peak drawing and feeding power from prosumers. Moreover, the day ahead, intraday and frequency containment reserve (FCR) markets are incorporated to the capacity mechanisms to evaluate their compatibility in the context of the Dutch power markets.

The advent of smart energy systems enables prosumers to become active participants in the market and aid in the grid's management. Thus, the approach of this thesis is to simulate prosumers' response to economic signals and evaluate the effects in a low voltage test feeder. To achieve this, the work develops on an existing smart charging algorithm that optimizes the components of the smart energy system. The system is composed of a multi port converter that incorporates a PV maximum power point tracking device (MPPT), a bidirectional EV charger, and a bidirectional battery energy storage (BES) charger; additionally, the grid is connected to a heat pump and load from appliances, which are non-flexible. The distribution network is IEEE's European low voltage test feeder, which is comprised of 55 households.

The techno-economic feasibility evaluation is done by benchamarking the capacity mechanisms against an energy tariff in two scenarios: winter, and summer. The benchmark results indicate that aligning prosumers with only an energy tariff leads to congestion in the feeder. In response, all capacity mechanisms evaluated were effective at managing congestion if properly designed, although, some restrict prosumers more than others. The hard constraint made prosumers lose the most load, and the total cost incurred by the prosumers in the feeder was greatest with the capacity subscription. The peak tariff had the lowest cost of lost load, and the least overall costs, consequently, the peak tariff was chosen to incorporate the day ahead, intraday and FCR markets to it. The incorporation of day ahead and intraday markets decreased the exposure to imbalance costs under the assumption that new forecasts with better accuracy were available one time step (15 min) before delivery.

The incorporation of FCR increased the exposure to imbalance costs due to deviations from the day ahead schedule. Furthermore, FCR with the peak tariff showed conflicting incentives, i.e., the peak tariff reduces the amount of reserved power for balancing regulation, else if full available power is reserved congestion increases. The results of this thesis point towards the potential that prosumers' demand response will have in shaping future decentralized energy systems, however, the market mechanisms in place need to be properly designed to ensure economic feasibility and resolve conflicting incentives between markets such as balancing and local congestion management.

ACKNOWLEDGEMENTS

Estoy profundamente agradecido con mis padres, mi hermano y familia, quienes siempre han creido en mí y me han apoyado incondicionalmente a procurar mis anhelos. A pesar de la distancia, su presencia y enseñanzas siempre han estado cerca de mí.

A Emma por, igualmente, creer en mí y motivarme a seguir adelante a pesar de obstáculos y dudas en el camino. Gracias por compartirme y enseñarme que la gentileza hacia uno mismo es el mejor antídoto contra la incertidumbre.

I want to thank Wiljan Vermeer for being my weekly supervisor and guiding me through out the whole process of developing my thesis. The discussions we had and his feedback have have been instrumental for sharpening my understanding and completing this work. Moreover, I want to thank Gautham Ram Chandra Mouli for supervising my thesis and constantly pushing myself by in-depth questioning the core of my work. This has been a learning experience that has shaped the foundations of what is to come in my professional career. Furthermore, I want to thank prof. Pavol Bauer for giving me the opportunity to do my thesis in the research group, as well, as been the chair of my committee. Thanks to Aleksandra Lekic for taking the time to be a member of my thesis committee.

Finally, I want to thank all the friends I have made in The Netherlands. Thanks to my Dutch friends for always welcoming me and inviting me into your way of life, rowing, sailing, and of course borrels. Thanks to my international friends for the countless conversations that we've had, it was been truly enriching to learn from different cultures, perspectives and backgrounds. It has been quite journey.

CONTENTS

ACRONYMS

RES Renewable energy sources

LCOE Levelized cost of energy

PV Photovoltaic

EV electric vehicle

HVAC Heating, Ventilating and Air Conditioning

TSO Transmission system operator

DSO Distribution system operator

DG Decentralized generation

HV High voltage

MV Medium voltage

LV Low voltage

SO System operator

BRP Balance responsible party

LLD Load limiting device

PTU Program time unit

BES Battery energy storage

MPPT Maximum power point tracking

SoC State of charge

AC Alternating current

DC Direct current

FCR Frequency containment reserve

aFRR Automatic frequency restoration reserves

mFRR Manual frequency restoration reserves

1 INTRODUCTION

1.1 RESEARCH GOAL STATEMENT

To investigate, evaluate and compare the techno-economic feasibility of novel energy market mechanisms that incentivize the involvement of prosumers in demand response and congestion management schemes.

1.2 RESEARCH QUESTIONS

The research approach is based on the goal statement in the previous section, for which the following research questions shall be answered.

1. What market mechanisms incentivize prosumers' demand response and congestion management in a future decentralized generation system?
   - What are the main challenges that can potentially be solved with prosumers' demand response and local congestion management?
   - What causes congestion in a low voltage feeder, and how is it expected to increase (or decrease) with more electrification, e.g., electric vehicle charging and electric heating?
   - What is the current state of energy markets (particularly the Dutch market), and what are the main considerations for aligning prosumers with energy markets assuming smart energy systems are in place?
2. What effects do prosumers with smart energy systems have on the low voltage feeder?
   - What are the main components of smart energy systems that prosumers might adopt in the near future?
   - How can the control in the smart energy system be formulated as an optimization problem?
   - How can the integration of prosumers' smart energy systems with a low voltage feeder be modeled?
3. What case study can evaluate and compare the effectiveness at managing congestion of the energy markets investigated?
   - What are the assumptions and input data of the case study?
   - What is the benchmark for congestion in the feeder based on the case study?
4. What are the metrics used to evaluate the market mechanisms for techno-economic feasibility?
   - How to expand the formulation of the optimization problem to incorporate the market mechanisms investigated?
   - How to determine the main parameters needed to model the market mechanisms?
   - What is the market mechanism that performs best in the case study used?

5. Is it feasible and convenient to integrate the day ahead and intraday market with the best performing market mechanism in order to minimize imbalance costs incurred by prosumers?
   - How do forecast errors impact on schedule deviations that incur an imbalance cost?
   - How can the schedules and procedures of the day ahead and intraday market fit together with the best performing market mechanism?
   - What are the imbalance cost reductions (if any) achieved by this incorporation?
6. Is it feasible to add the involvement of prosumers to the frequency containment reserve market on top of the best performing mechanism, day ahead and intraday markets?
   - What are the implications that providing frequency containment reserves have on the committed schedules to the day ahead and intraday market?
   - Are there any conflicting incentives between balancing regulation at a transmission level and congestion at a distribution level?
7. What are the main conclusions drawn from this work and what further research can be proposed?

2 LITERATURE REVIEW

The literature review investigates novel energy systems with a high penetration of RES and decentralized generation, outlining the relevant context to demand response schemes where prosumers are involved by providing flexibility through economic incentives. This is presented in four subsections. In section 2.1, the main challenges that such energy systems pose to current networks and their causes are discussed. In section 2.2, some potential methods in which prosumers can be aligned to the market mechanisms for their involvement are explored. In section 2.3, a brief description of the current electricity market and its sub markets is presented.

2.1 MAIN CHALLENGES OF DECENTRALIZED GENERATION

2.1.1 Electrification and increase in load demand

The human civilization is producing evermore complex societies that, among other things, increasingly demands more energy to satisfy its needs. Along with these increases in demand, the systems and infrastructures that provide it are growing in complexity too. The second half of 18th century brought a massive shift to human societies; the light bulb and steam engine changed the role energy would play in development and economic growth. For the most part fossil fuels have been the protagonists of energy demands until their effects on the environment and its depletion became clear; this has resulted in about 0.5 trillion tonnes of oil equivalent barrels extracted worldwide and 1.2 trillion tonnes of carbon dioxide emitted worldwide, since the Industrial Revolution [15].

The late 20th and beginning of the 21st century marks the energy transition towards sustainability where electricity is becoming the main energy carrier. On one side, there has been a rise on all kind of appliances and tools that are steadily demanding more energy. The technology explosion and internet of things is an example where data centers, crypto currency mining, personal computers and mobile phones have been requiring vast amounts of electricity in recent years.The annual energy consumption from Bitcoin in 2018 was around 45.8 TWh [45]. The battery capacity of a Nokia 3310, released in 2000, was 900 mAh while the iPhone 12 Pro Max, released in 2020, has a 3687 mAh capacity [19, 18] . On the other side, there are two sectors that have been migrating from fossil fuels to electricity as their means to perform work due to the carbon emissions they cause, transport and heating [33].

The transport and residential building sector accounted for 23% and 10% global emissions in 2018, respectively [23]. Passenger and light duty vehicles for land transportation are the biggest emitters, hence, they have had a substantial shift towards electrification in the past decade. The global electric vehicle (EV) stock went from 0.02 million in 2010 to 4.79 million in 2019, as per Figure 2.1a. Electric heating has not had such an increase as electric vehicles, however, according to IEA's Sustainable Development Scenario a strong trend should be expected for the upcoming decades if emission targets are to be met, Figure 2.1b.

All of this means that the electricity sector is under increasing pressure to meet the global needs of a strong electrified society where load demand is rapidly grow-

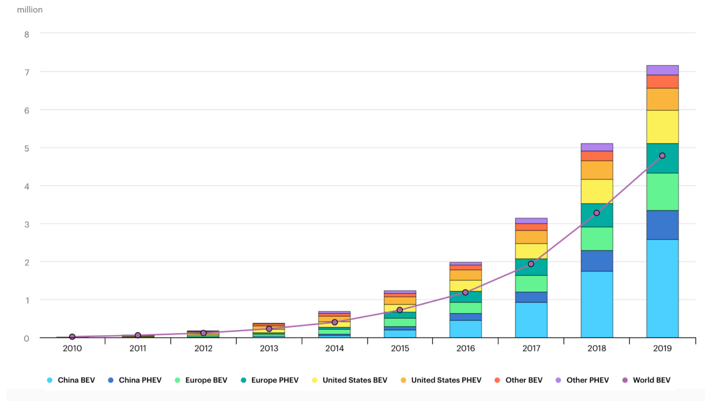

(a)

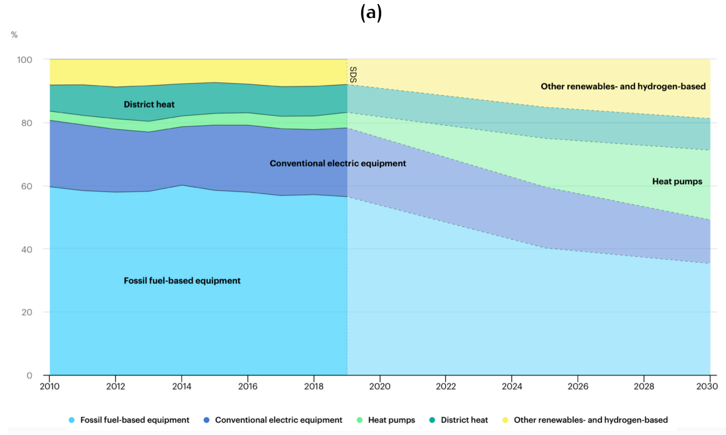

(b)

Figure 2.1: Electrification of sectors. (a) Global electric car stock,[23]. (b) Heating technology sales in the Sustainable Development Scenario,[24]

ing. The global electricity demand increased by 75% from 2010 to 2019, whereas, the fossil fuel demand increased by 20% in that same period [11]. The sector needs to expand enough to provide the electricity demand and accomplish it in a sustainable manner to ensure environmental goals. There is no point in electrification efforts if the electricity is generated with fossil fuels, therefore, an increase of renewable sources penetration is the second pillar of the energy transition.

2.1.2 Intermittent renewable energy sources

The rise of renewable energy sources (RES) has been the result of direct efforts to mitigate the adverse effects of fossil fuels, resulting in great costs reduction of renewable technologies, causing further renewable sources penetration. In recent years the levelized cost of electricity (LCOE) for photovoltaic (PV) and wind technologies has fallen below their fossil fuel counterparts [17]. Additionally, it has made small scale consumers (i.e., households and small buildings) to be involved in the sector as prosumers too, since the LCOE of PV is in many cases less than the retail price [31]. This is shifting the trend from a paradigm of centralization towards one of decentralization. Furthermore, RES have a massive potential to supply many times the global energy needs, in some estimations the potential is more than 3,000 times the current energy demand, figure 2.2 [10]. Although this potential is promising, there are several serious constraints and challenges to overcome before a full energy transition can be achieved. [34] argues that there are various conflicting estimations for RE potential, except for hydro, due to constraints' considerations. RES are, mostly, uncontrollable and intermittent by nature since they are energy flows rather than energy stocks. Hydropower, which is controllable, has had a vast growth in installed capacity in the last century and is near to its limit in terms of geographic constraints, however, PV and wind are far from their limit.

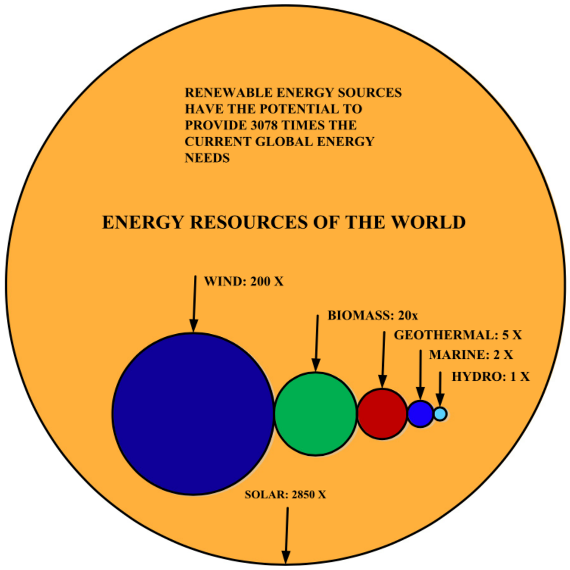

Figure 2.2: Global energy resources [10]

PV and wind generation are dependent on a multitude of variables, such as weather, location and time of the day, hence, they are intermittent in a seasonal and daily basis. Plus, these sources are unpredictable with great accuracy due to the reliance on forecasting of complex systems, like the weather. In addition to generation, the transmission and distribution of the electricity to the end user is more complex as these sources have more penetration. The proliferation of PV on the rooftops of prosumers enables the decentralization paradigm. However, the coordination between large-scale producers and small-scale prosumers is increasing complexity and requires more effort to maintain due to greater stochasticity of the system's balance between generation and demand [7]. All of these factors result in higher levels of congestion in the electricity grid that need to be resolved. There have been several schemes proposed for future decentralized energy systems to resolve said issues, these are reviewed in next sections.

2.2 FUTURE DECENTRALIZED ENERGY SYSTEMS

2.2.1 Congestion in the network

Generally, the network infrastructure consists of high voltage transmission lines that transport electricity from remote generation locations to substations near consumers, medium voltage distribution lines from substations to low voltage feeders, and from the feeders to each household for end consumption. Together with various power devices, transformers scale voltage down (or up) along the supply chain to ensure that the power flow is within the working capacity of devices. Congestion occurs when devices (i.e., transformer and cables) from the network surpass their thermal capacities, overloading regions of the system. Frequent instances of overloading lead to increased degradation of the network's assets and reinforcement is necessary, therefore, congestion management is key to maintain the network operational [22].

The system's operators are responsible, among other things, for maintaining the balance between supply and demand, and to ensure technical integrity of the network. The transmission system operator (TSO) is responsible at a transmission level and the distribution system operator (DSO) is responsible at a distribution level. The scope of this review is focused on the low voltage level, between the DSO and feeder connected to the households. The rise of EV's, electric heat pumps and the reversed power flow of PV's from prosumers can result in higher congestion at the low voltage feeder level that needs to be managed [22]. The architecture of the feeder may affect the nature and magnitude of congestions in a decentralized energy system with a high amount of decentralized generation (DG). In a densely clustered network, such as in the Netherlands, congestion could be a severe issue for MV/LV transformers. [55] shows that by 2040, in the Netherlands, the expected increase in load demand and DG could overload 87% of these transformers and 34% of the distributions lines.

It is essential to address current and expected congestion issues in the grid. Traditionally, the power system has been designed with a top-down approach where the focus was to ensure capacity for peak loads and conventional flexibility sought to match loads by varying the controllable generation upon unexpected failures or disruptions from the power system's components [32]. The conventional paradigm would mean to reinforce the network to accommodate new higher peak capacities, however, this may be considered redundant since peaks (generally) occur in short a duration throughout the year. Additionally, reinforcement will need huge investments and will be a slow process, and might not even meet the increasing peak demand [32, 30, 40, 20]. Hence, the operators face the challenge to continue with the same paradigm of grid reinforcement or change the paradigm and seek smart solutions that are tailored for RES and DG integration. An efficient method is to value consumers' flexibility through local congestion management and demand response schemes [30, 37].

2.2.2 Congestion management

The core problem for LV congestion is that prosumers expect availability of electricity at all times regardless of the network's status, in other words, demand is inelastic. Furthermore, the small scale generation from installed PVs is fed to the grid whenever it is available (assuming no storage), again, disregarding network's congestion. In this context, there is a high value to be gained if prosumers' loads (and generation) can be shifted to less congested schedules without curtailing overall loads Figure 2.3.

In order to achieve the flexibility in demand, there are two broad approaches: 1) direct physical measures, e.g., active power curtailment, automated demand response, graceful degradation, 2) indirect incentive-based mechanisms that motivate prosumers to adjust their demands, i.e., price based [21, 20, 40]. The latter are in line with a liberalized electricity market rationale. Among the incentive-based mechanisms, there may be a central control entity that processes the network and prosumers' information for dispatching through complex bids, or a decentralized approach to sort locally the intended goals of the involved entities. A decentralized view is increasingly desirable because it reduces the need of perfect information and increased computational complexity that would burden a central operator [22, 39].

Currently, one of the central issues is that the retail prices that small scale prosumers pay do not reflect the real time status of the network. It is important to distinguish between two different objectives procured by the system operators, which

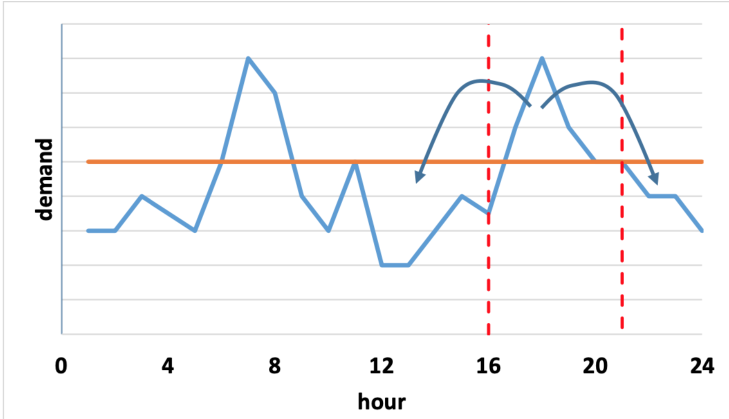

Figure 2.3: Example of load shifting,[7]

are not properly reflected by the retail prices: system's balance and congestion management. First, the retail prices do not expose the prosumers to the market's scarcity or abundance signals that the wholesale electricity prices, in principle, do [29]. Second, retail prices also fail at reflecting the true costs incurred by prosumers due to grid congestion [39]. Therefore, there is no motivation for prosumers to take part in balancing the system nor managing congestion. [29] showed that prosumers can be aligned with wholesale prices to better reflect scarcity signals, however, [40, 44] argue that simply aligning such prices to prosumers may lead to high levels of congestion. This is a result of energy tariffs being inherently inefficient at valuing capacity availability and flexibility [38]. In response to this, next section describes novel market mechanisms that aim to offer a solution to current price inefficiencies.

2.2.3 Market based mechanisms

Due to the increasing interest on the potential benefits of flexibility, several mechanisms have been proposed that veer away from conventional retail pricing to achieve efficient demand response from prosumers [41, 28, 32]. These mechanisms can be divided into explicit and implicit. The former refers to committed capacity that can be traded in flexibility markets (usually, via an aggregator) in exchange of a remuneration. The latter consist of price signals where prosumers are incentivized to modify their behavior to optimize costs (manually or automatically) [42].

[28] conducted a literature review condensing the concepts, models and clearing methods of local flexibility markets that have been proposed. The key insights (for this work) are four. 1) There are three types of flexibility to be traded; balancing for the TSO at a transmission level, balancing at a distribution level between TSO and DSO, and voltage control and congestion management for the DSO at a local level. 2) The five main features to consider in a local flexibility markets are: power flow direction, rate of change of power capacity, starting times and its triggers, duration and location of the distribution nodes. 3) The participants of local flexibility markets (at a distribution level) are: DSO, a market operator, aggregators and balance responsible parties (BRPs); not all proposed mechanisms necessitate BRPs. [40] argue that it may be more efficient to have prosumers directly trade in the market without an aggregator. 4) The local flexibility market can work in parallel with other existing markets, i.e, day ahead and intraday.

There have also been various mechanisms proposed regarding price based incentives. The mechanisms can be differentiated between volumetric tariffs (energy based) and capacity tariffs (power based), among these, they can be static or dynamic depending on the time of use, and based on location (regional/national or local) [30, 41, 44, 3, 8]. [38] propose power trading in the day ahead market instead of energy trading to reduce excessive costs and scheduling failures due to increasing resolution of schedules.

[39] evaluates three different designs: integrated market, wholesale energy pricing and locational energy market; they conclude that an integrated market shows the best results, however, it is infeasible due to perfect information requirements, although, locational pricing can have similar results unlike wholesale. [29] provide a market alignment indicator that compares the results (against a benchmark) of aligning prosumers to the wholesale energy market and indicate that the wholesale market can lead to congestion. [2] asses the effectiveness of capacity markets where a high portfolio share of RES is present and conclude that these markets can reduce consumer costs, improve adequacy and are more efficient that strategic reserve.

[8] proposes a capacity subscription where prosumers subscribe to a peak that is guaranteed and after that threshold, they can be subject to curtailment through limiting load devices (LLDs) or are able to buy excess power at a higher price. [3] further expand on the previous mechanism and evaluate a static and a dynamic capacity tariffs, in the context of a grid tariff proposed by the Norwegian regulator. They point out that in a grid tariff prosumers pay an excess price (or value of lost load) when they surpass the subscribed amount even if there is no capacity scarcity, hence, the dynamic tariff is a better alternative in the presence of storage; investment of a battery and presence of an EV were not included.

[44] analyzes the effectiveness of an energy tariff, capacity tariff (with peak and tier tariffs) and a flexibility market in the context of conflicting interest between grid balancing and congestion management, They compare their ability to prevent congestion and value of flexibility in the imbalance market. The results assert that energy tariffs do not reduce congestion but rather shift the time of occurrence. Capacity tariffs and the flexibility market both prevent congestion, however, the loss of value for the imbalance market strongly depends on the design of the mechanisms and behavior of the grid, i.e., tariff prices, day ahead schedule and EVs' penetration in the system.

2.2.4 Demand response schemes

In order for demand response to be successful at tackling the challenges discussed previously, proper financial incentives are not the only aspect to be considered but integration of technologies in a so-called smart grid. There are some key features that are expected from prosumers that will enable demand response in a smart grid. Generally, a prosumer could encompass: smart metering for alignment with real time circumstances of the grid, power generation (mostly PV), a battery unit for storage, an EV (or several), heat storage, power electronics for AC/DC conversion, appliances and a smart optimization control that would determine the power flow based on internal (load demands) and external (incentives) factors [33, 32, 28]. Figure 2.4 illustrates the integration. The adoption of these features greatly depends on a financial decision from the prosumers' standpoint [29], however, even if not all are adopted the fundamental concept is that the proliferation of information and communication technologies (ICT) and power electronics can optimize, bottom-up, the power flow of smart grids.

Conventionally, small-scale load demand has been inelastic characterized by a passive role from consumers. Due to the rise of electrification and new technologies (previously reviewed), prosumers are now able to take an active role. To this end, there is a distinction to be made between fixed and flexible loads from the pro-

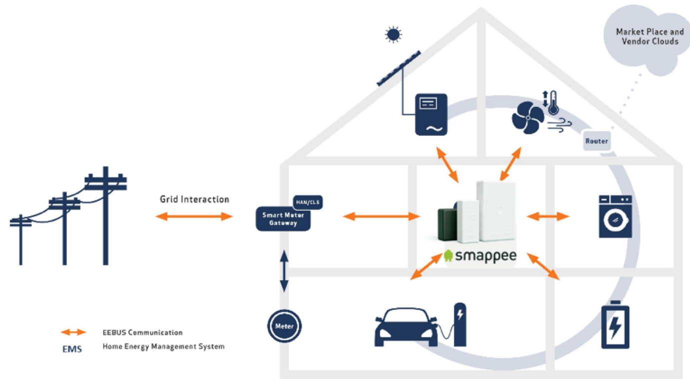

Figure 2.4: Illustration of smart grid integration

sumers' comfort side. The traditional appliances in residential buildings would be considered fixed loads since they are part of the daily patterns of demand from prosumers and rarely contribute to the issues posed by electrification and intermittent sources of new systems. Flexible loads can be shifted based on financial incentives and individual preferences, such as, EVs, heat pumps, and electrical heating ventilation and air conditioning (HVAC) [21, 32, 33].

The preferences of each prosumer may vary widely, thus, a properly designed demand response scheme would assign value to the reliability preferences of each prosumer making it a private good rather than a common good where actors are subject to involuntary load shedding [7]. Additionally, demand response can provide flexibility to other markets of the energy sector, e.g., ancillary services to the balance market. For small-scale prosumers, batteries and EVs open an opportunity to provide power to the grid when it is needed in exchange of remuneration or bypass high grid prices and provide internally; smart charging and discharging has proven to be economically efficient even considering the degradation costs of the batteries [56]. The International Energy Agency Outlook [25] states that around 40% of global energy consumption corresponds to buildings, hence, there is a vast value to be gained by integrating them in a smart grid. [32] argues that large-scale storage will remain with a small contribution to power system in the short and mid term, whereas, small scale integration has a higher impact in the short term due to lower overall costs. In consequence of it, there has been a growing interest introduce demand response around the globe and in some case it has already been successfully introduced.

[14] evaluated flexibility values for congestion management of four pilots that have been conducted in the Netherlands.

1. "Your Energy Movement" (YEM) consisted of a two phase pilot where consumers were provided of a smart energy management device where they could monitor their consumption and dynamic price tariffs. The first phase (in 2013) focused on washing machines with little results, the second included batteries, PV and heat pumps. The main results were that dynamic energy tariffs alone can lead to higher congestion due to consumers consuming power at the lowest prices at once, and that active monitoring involvement of consumer was challenging due to knowledge levels from participants.

2. "FlexPower" centered solely on EVs. Participants contracted a static profile with an on-peak hours capacity (2h) and off-peak hours capacity (22h) with a 50% reduction and 25% in capacity, respectively. Participants could overturn

their contract at on-peak hours at a premium cost. This pilot showed successful results, 46% of peak capacity was reduced, however, this static method can potentially shift capacity demand immediately after on-peak hour all at once creating congestion at a later period.

3. "PowerMatching City" evaluated "PowerMatching" technology, where and agent-based market equilibrium is reached by aggregating all stakeholder (participants, network and market) and solving the optimization problem to calculate the marginal pricing of assets. Households were provided with smart appliances, heat pumps, PVs, EVs (and a wind turbine was added to the project); they could decide to automatically, semi-automatically or manually manage their loads. The project showed that consumers were willing to change their behaviors, however, it is a challenge to fairly distribute benefits among all stakeholders.

4. "Energiekoplopers" used USEF, a flexibility market framework, where participants were given smart appliances, heat pumps, PVs and fuel cells; they could trade flexibility in a day-ahead and intraday market with the DSO and a BRP. The main results were that around 67% of flexibility purchased was delivered and that at some points there were conflicting interest between the DSO and BRP.

2.3 LIBERALIZED ENERGY MARKETS

2.3.1 Dutch market

By the end of the 20th and beginning of the 21st century, many countries opted for a liberalized electricity sector based on neoliberal economic theory that argues efficiency and innovation through free market competition, rather than a strong involvement form the State. A key component of the liberalized sector is unbundling the previous, highly integrated structure of the sector. The restructuring aims to provide a competitive and "fair playing field" to all parties involved, however, the nature of the sector forms a natural monopoly for the network's infrastructure where the State takes ownership. Europe has taken this market paradigm, furthermore, the Dutch market is a fairly rigorous case of a decentralized electricity market [27].

The sector in the Netherlands can be divided into two main components: a physical, technical component and an institutional, economic one. The former entails the power flow in the system, the generation, transmission and distribution to end consumers, and all the necessary engineering equipment. The latter encompasses the actors involved in the control and operation, producers, consumers and intermediaries, and the venue where they interact, the market. TenneT, State owned, is the TSO responsible for the balance between injections and withdrawals of power in the system, management of the transmission network and management of import/export capacity. The DSOs, owned by local governments, are responsible for the distribution networks, balance, congestion management and voltage control at a distribution level.

The differentiation between transmission and distribution is based on the lines' voltage; the TSO manages high voltage (>110kV) and the DSOs the medium and low voltage (<110kV). The standard frequency of operation in the European interconnected countries is 50Hz [1]. Additionally, producers are private companies that own generation plants and can sell electricity directly to large consumers or small consumers through retailers. The transactions take place in the wholesale market, which can be subdivided into: bilateral market, power exchange, balancing market and import/export auctions; Tennet operates the last two. Around 85% of electricity is purchased via confidential bilateral contracts, the remaining is traded in the spot market (APX) . Figure 2.5 provides an illustration of the sector.

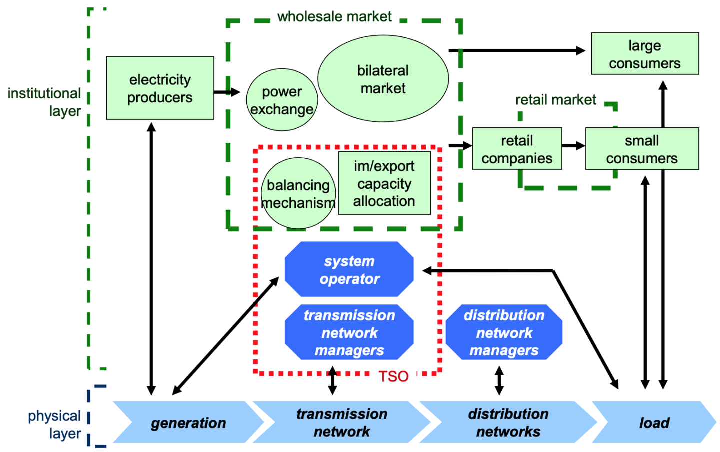

Figure 2.5: Diagram of electricity system,[27]

2.3.2 Power exchange

The power exchange is divided into sub-markets: forward and futures, day ahead, intraday, and balancing market. Forward and futures are contracts for physical delivery of the commodity and speculative "papers" for price risk hedging, respectively [16]. The spot market is formed from the three remaining sub-markets. In the day ahead electricity is traded based on the marginal costs of generation, where a single clearing price is achieved in a quarterly basis (15min) in the Dutch market one day prior to delivery. The balancing market consists of reserve procurement and imbalance settlements in a real time frame [1, 27]. Figure 2.6 provides a schematic illustration of the time frames.

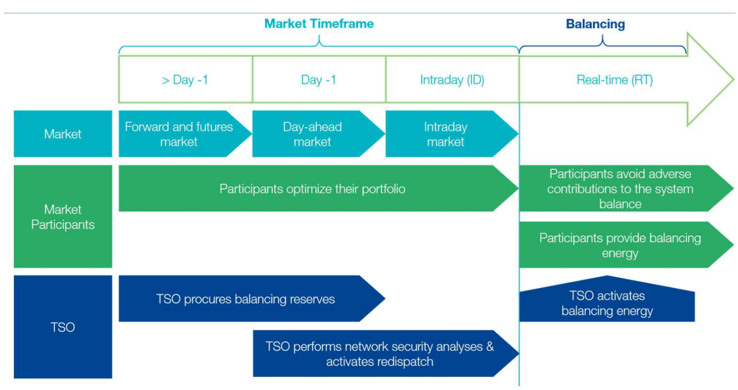

Figure 2.6: Wholesale market time frame [49]

Tennet provides an annual market review on the developments of the Central Western European countries, particularly the Dutch and German market [49]. Following are some relevant insights (for this work). In the Netherlands the electricity price is strongly influences by the natural gas plants due to their relatively high portfolio share. The intraday market provides a venue for participants to optimize their positions of the day ahead market against load and generation forecasting errors, and unexpected outages; this are continuous auctions where no single price per hour is set, unlike in the day ahead market. In recent years the intraday market has had a substantial increase in trading volume due to the growing penetration of RES in the electricity share portfolio; 2019 saw a 57% increase of energy traded compared to 2018. Figure 2.7a shows this trend and the fact that most intraday trades occur towards the evening. Since day ahead and intraday prices are correlated, it is useful to measure their delta. Historically, day ahead prices have been higher than intraday for more hours in a year. Figure 2.7b illustrates the delta distributions.

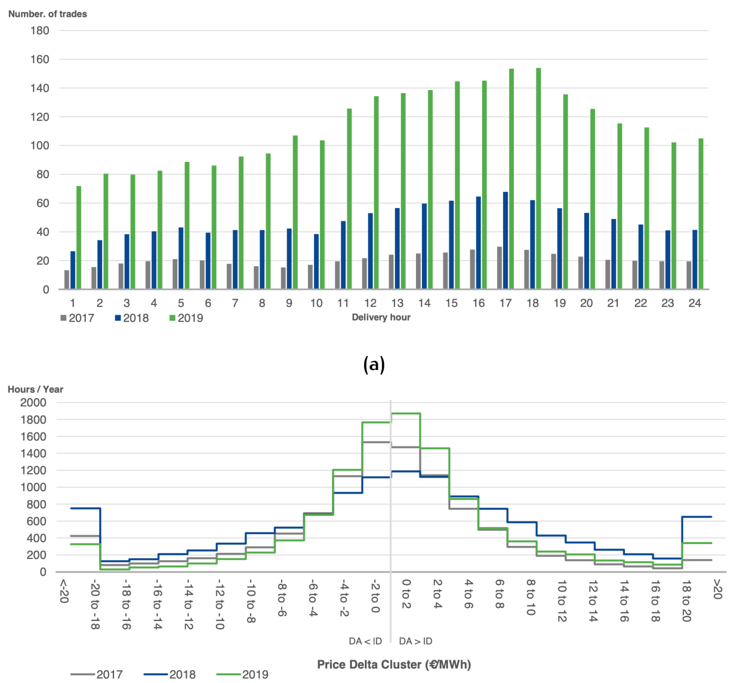

(a)

(b)

Figure 2.7: Intraday market,[49]. (a) Intraday trading volumes. (b) Day ahead and intraday price delta.

2.3.3 Balance market

Due to the fact that it is not yet economically feasible to store electricity at a large scale in the network, all commodities traded in the market need to be generated and consumed almost instantly. Therefore, all users of the network are considered "program responsible", although, there are only a few dozen large users (producers, consumers or suppliers) that actually bear this responsibilities, while the rest of the users transfer their program responsibility to them. These are the BRPs, who are financially responsible to maintain the balance between demand and supply. BRPs settle any mismatches between demand and supply on a real-time basis against the imbalance prices from the market where Tennet is the operator [49]. Participants can provide ancillary services (through their BRP) through bids and the TSO controls the activation of the winning bids. The design of the balancing market entails three main pillars: balancing responsibility refers to the planning and scheduling of generation and demand a day before delivery until the closing gate, balance service consists of the bidding that the TSO can choose to activate, and imbalance settlement where the deviations from the energy program are set according to the imbalance prices for any given program time unit (PTU) [46, 27]. Figure 2.8 provides an overview of the balancing market.

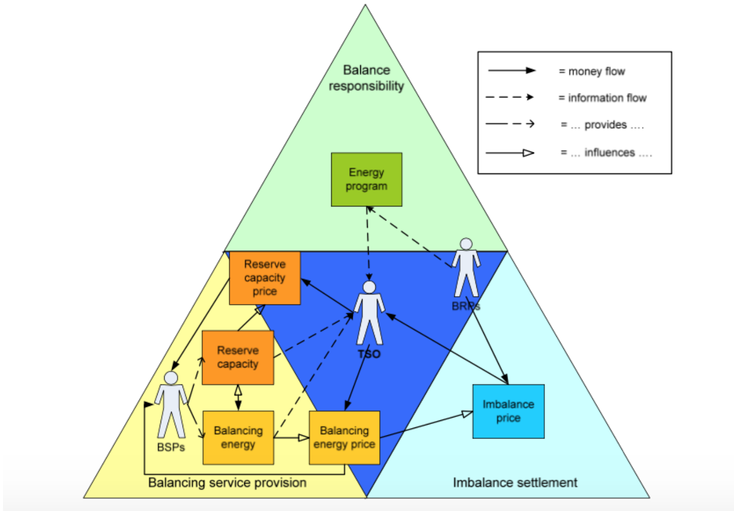

Figure 2.8: Schematic overview of balancing market, [27]

There are two main distinctions between the balancing services provided: balancing energy and reserve capacity. The first is dispatched via up or down regulation to ensure a real time balance between supply and demand for every program time unit (PTU). The second are procured reserves through contracts of specific duration before delivery. The TSO contracts the option to use the reserves for control of the system [6]. The balancing reserves are subdivided into: frequency containment reserves (FCR), automatic frequency restoration reserves (aFRR) and manual frequency restoration reserves (mFRR); formerly named primary, secondary and tertiary control, respectively [48]. These reserves are procured to mitigate deviations from the 50 Hz standard. The interconnected networks need to maintain synchronicity around the standard frequency, hence, the contribution of the Dutch connections (3.7% of the total network) is the reference for the amount of reserves needed for dispatching at any given moment. In 2021 the minimum volume of reserves needed are 114 MW, 300 MW and 1 005 MW for FCR, aFRR and mFRR, respectively [52].

Additionally to frequency control the TSO needs to control the reactive power flowing through the network. Reactive power does not add to the active power flow, however, it strongly impacts on the voltage levels within the network. The operator has several sources to control for reactive power, such as, shunt sinks and capacitor banks, nevertheless, sometimes it may need to request generator or power park modules for control. Voltage control is divided into primary and secondary, the former is designed to activate almost immediately and automatically in the presence of any disturbance, and the latter is performed solely by the operator to optimize the use of stationary facilities. Voltage control strongly depends on the location of disturbance, consequently, TenneT makes a regional estimation of the amount needed for the coming year and issues an invitation to tender for the supply of voltage control by generators [50]

3 SMART ENERGY SYSTEM AND GRID MODEL

This chapter describes the smart energy system and the distribution network model employed. The former was developed by [56], and the latter is based on [26]. These two are integrated together to study the behavior of prosumers in response to different market mechanisms, and the subsequent effects on the grid at a low voltage level due to those behaviors. The chapter is composed of 4 sections. In section 3.1 the components of the smart energy system are outlined. In section 3.2 the formulation of the system as an optimization problem and its constraints is laid. In section 3.3 the time frames and control techniques are detailed. In section 3.4 the distribution network model and the integration with the smart energy system are presented.

3.1 COMPONENTS OF THE SMART ENERGY SYSTEM

This section was not developed as part of the thesis, however, it is presented as reference since it has been used to develop the work of this thesis.

As discussed in section 2.2, there has been an accelerating change in the paradigm of the energy sector. Energy systems are shifting towards a more decentralized approach where players of smaller scales are becoming more prevalent and relevant. In this context, the smart energy system provides management of the various components and power flows for a typical prosumer within a decentralized system with high penetration of RES. The system consists of a multi port converter that incorporates a PV maximum power point tracking device (MPPT) [5], bidirectional EV charger [35], and a bidirectional battery energy storage (BES) charger, DC flows.

Additionally, the grid is connected to a heat pump and the load from appliances, for AC flows. The system is managed by the smart charging algorithm based on inputs (forecasts and economic signals) and outputs power levels for the PV, BES, EV and exchange with the grid. The optimization is a cost minimization that considers inner constraints of the system, such as, state of charge (SoC), degradation of BES and EV, and availability of the EV. The economic signals may vary depending on the markets in place, e.g., energy tariffs, capacity mechanisms, ancillary services and flexibility markets. Figure 3.1 illustrates a schematic representation of the system.

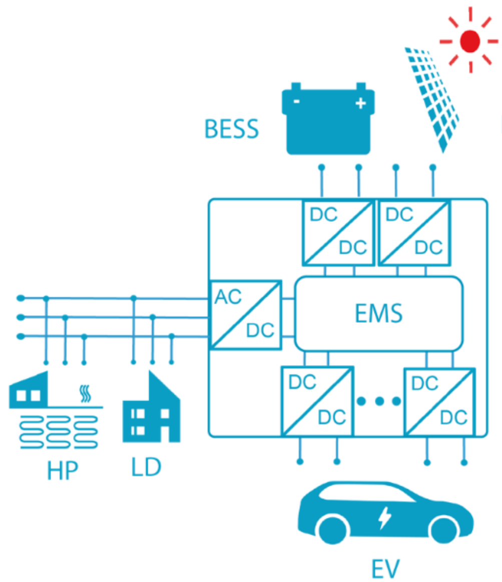

Figure 3.1: Smart energy system's diagram [56]

3.2 FORMULATION OF THE SYSTEM AS AN OPTIMIZATION PROBLEM

This section presents the main functions that form the objective function of the optimization problem. The constraints of the model are not presented here, the complete model can be found in appendix A. Further reference can be found in [56].

3.2.1 Objective function

The objective of the smart charging algorithm is to minimize overall costs for the prosumer, hence the main objective function is formulated 3.1. The function consists of battery costs C_{BES} , EV costs C_{EV}, PV costs C_{PV}, grid costs C_{Grid} and revenue due to regulation C_{Reg}. This function is the basis for subsequent mechanisms and will be modified accordingly in following sections. In order to model the optimization problem, CONOPT4 solver on the Generic Algebraic Modeling System (GAMS) is used.

$$min(C_{Total}) = min(C_{BES} + C_{EV} + C_{PV} + C_{Grid} - C_{Reg}) \tag{3.1}$$

3.2.2 Battery costs

The battery costs C_{BES} are due to the operation of the Lithium-ion battery. These costs are calculated by subtracting the degradation of the battery ΔE_{BES}^{Total} to its initial capacity E_{BES}^{max}, both in kWh. The degradation model is taken from [57], and consist of a calendar and a cyclic aging per time step. The model is for a single Nickel-Manganese-Cobalt (NMC) cell and scaled up considering 14 cells in parallel and 100 in series. Thereafter, the value of the battery V_{BES}, in €/kWh, is determined as presented in [36]. It is assumed that the battery is in its first life V_{BES}^{new}, which ends at

80% of the initial capacity. The value of the second life of the battery V_{BES}^{2nd} is equal to 50% of a new one. The value of the battery is shown in equation 3.2 and the cost in .3, in €.

$$V_{BES} = \frac{V_{BES}^{2nd} - V_{BES}^{new}}{0.2} \Delta E_{BES}^{Total} + V_{BES}^{new} \tag{3.2}$$

$$C_{BES} = V_{BES}^{new} E_{BES}^{max} - V_{BES}(E_{BES}^{max} - \Delta E_{BES}^{Total}) \tag{3.3}$$

3.2.3 Electric vehicle costs

The EV also has operational costs due to driving and due to providing power to the grid (V2G). The driving costs are not part of the optimization and hence outside of the control, however, they are accounted for as the whole system is updated in subsequent time steps (discussed in section 3.3). The costs C_{EV} caused by providing V2G power have the same treatment as the battery in .1.1 above. The equation for the value of the EV (for V2G) is 3.4 and for costs is 3.5.

$$V_{EV} = \frac{V_{EV}^{2nd} - V_{EV}^{new}}{0.2} \Delta E_{EV}^{Total} + V_{EV}^{new} \tag{3.4}$$

$$C_{EV} = V_{EV}^{new} E_{EV}^{max} - V_{EV}(E_{EV}^{max} - \Delta E_{EV}^{Total}) \tag{3.5}$$

3.2.4 Photovoltaic costs

The PV costs C_{PV} are levelised per kWh, as per [43] the parameter used is $\lambda_{PV} = 0.03$ €/kWh. The cost of providing PV power for the prosumer are calculated with equation 3.6.

$$C_{PV} = \sum_{t=1}^{T} P_{PV}(t) \Delta t \lambda_{PV} \tag{3.6}$$

3.2.5 Grid costs

The grid costs C_{Grid} are the result of system's grid exchange, either drawing $P_{Grid}^{Buy}(t)$ or feeding $P_{Grid}^{Sell}(t)$. The power fed/drawn in each time step are subject to a dynamic energy tariff, in €/kWh, $\lambda_{Buy}(t)$ and $\lambda_{sell}(t)$, respectively. The selling price is 50% lower than the buying price in order to simulate a scenario where prices for the prosumer are a function of demand and supply; this also provides arbitrage to ensure that $P_{Grid}^{Buy}(t)$ and $P_{Grid}^{Sell}(t)$ are not non-zero simultaneously [56]. These energy tariffs, in principle, optimize to feed energy at high prices (energy scarcity) and draw from the grid at low prices (energy abundance). Equation 3.7 shows the calculation of the grid costs.

$$C_{Grid} = \sum_{t=1}^{T} P_{Grid}^{Buy}(t) \lambda_{Buy}(t) \Delta t - \sum_{t=1}^{T} P_{Grid}^{Sell}(t) \lambda_{Sell}(t) \Delta t \tag{3.7}$$

3.2.6 Regulation revenue

The revenue C_{Reg} is the result of acting as a frequency containment reserve (FCR) by reserving power capacity for primary frequency regulation. It is assumed that an aggregator will be the intermediary between the prosumer and the FCR market, and it will bundle together several prosumers to meet power requirements. Up/down regulation prices are $\lambda_{Up}(t)$ and $\lambda_{Down}(t)$, respectively. $P^{Up}_{Reg}(t)$ and $P^{Down}_{Reg}(t)$ are the reserved power capacity for up and down regulation, respectively. Additionally, $\eta_{inv/ch}$ are the efficiencies of the inverter and BES/EV chargers, correspondingly. The revenue is calculated with equation 3.8.

$$C_{Reg} = \eta_{inv}\eta_{ch} \sum_{t=1}^{T} (P^{Up}_{Reg}(t)\lambda_{Up}(t) + P^{Down}_{Reg}(t)\lambda_{Down}(t))\Delta t \tag{3.8}$$

3.3 TIME FRAMES AND CONTROL TECHNIQUES

The goal of the smart charging algorithm is to find the optimal schedule (as discussed in previous section 3.2 for all the relevant power flows in the system, which will result in a schedule for power exchange with the grid. The optimization window is for the 24 hours of the day at a 15 min resolution Δt, which coincides with each program time unit (PTU) of Dutch (and interconnected) markets. The system is fed with forecasts of the necessary parameters, e.g., loads, solar irradiance, EV availability and prices., to schedule to most cost efficient power levels. However, these forecasts are subject to errors due to their stochastic nature, and are even expected to increase in coming years as mentioned in chapter 2. The parameters and forecasts are further elaborated in the following chapter 4.

3.3.1 Moving horizon

In order to cope with forecast errors, a moving horizon predictive controller is put in place [56]. This control works on the basis that a new forecast with better accuracy (in principle) will be available every time step. In other words, the forecast for e.g., the load at $t - 24h$ will be considerably less accurate than the one for the same load at the time step previous to delivery $t - 15min$. This moving horizon ensures that the best power schedule will result from the most accurate information available at any given moment in time. The moving horizon will be tailored to the context in which of the market mechanisms the energy system is embedded, e.g., energy tariff, capacity tariff, day ahead and/or intraday. This allows the smart charging algorithm to be flexible and adapt to different market designs.

3.3.2 Real time control

Even with the moving horizon errors are still expected due to forecast inaccuracies and the difference in time resolutions between the optimization's time steps (15min) and real time; therefore a real time control is implemented. This real time control is a rule-based control operating on a 1min resolution. Its purpose is to maintain power balance at all times between the different components of the system and the system with the grid. The control works on top of the pre-optimized scheduled correcting the power errors P_{Error} at any instance. The error is calculated with equation 3.9.

For example, if the load at an instance t turns out to be larger than expected and the optimized schedule assigned the BES to supply the load (or part of it) the control will correct the discharging power P^{dis}_{BES} at a higher level, if available. If this control was not implemented, then all power deviations would have to be compensated with grid power P_{Grid}. Compensating with the grid may or may not be beneficial from a cost stand point, hence, the control compares the cost to the average cost for the 24h time window. If it is cost efficient grid power will be used, else if the BES and/or EV are available they will compensate. The availability of BES and EV depend on their power rating, SoC, and the power balance inside of the multiport converter. Lastly, at the end of every real time control time step the actual degradation of BES and EV are calculated and updated for future optimizations of the schedule at a 15 min resolution. Figure 3.2 illustrates the whole control scheme's flowchart.

$$P_{Error} = P^{fc}_{Load} - P^{ac}_{Load} - (P^{fc}_{PV} - P^{ac}_{PV}) \tag{3.9}$$

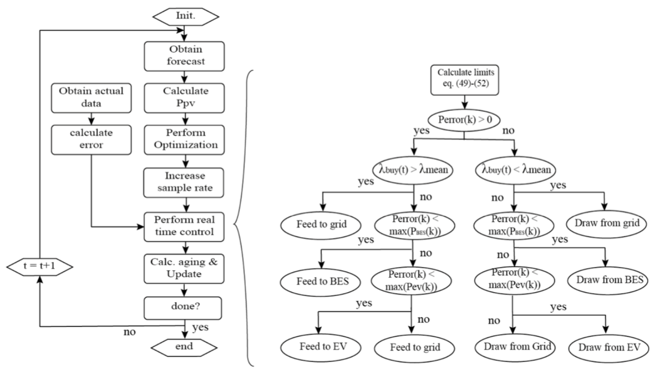

Figure 3.2: Moving horizon and real time control flowchart [56]

3.4 INTEGRATION OF DISTRIBUTION NETWORK AND SMART ENERGY SYSTEM

Once the smart energy system of prosumers has been defined, the effects of such systems in the grid at a distribution level need to be modeled. To achieve this, the IEEE European low voltage feeder [26] is employed as a grid model. Figure 3.3 shows the single line diagram of the low voltage distribution network. It is a radial feeder with 906 Buses consisting of 55 households connected with 3 phase cables. Each household has its own load and they are modeled as a constant PQ with a PF = 0.95, and a 25 A connection. The low voltage feeder is connected to a substation where a step-down transformer with 0.8 MVA capacity transforms a voltage of 11 kV into 0.416 kV at 1.05 pu. The test feeder is modeled using MathWorks' Simscape Electrical - Specialized Power Systems, in SIMULINK [9].

As stated, the purpose of the grid model is to study the effects, e.g., congestion in the feeder caused by a future decentralized paradigm. In this context, it is assumed that each one of the 55 households will have a smart energy system in place that will dictate how much power will be drawn/fed from/to the grid. Of course not all households will be the same, each one will have its own capacities, constraints and preferences. For example, some might have a bigger heating demand due to a higher household volume, which in turn, will allow for larger installed capacity of PV due to a bigger roof area. Some might have longer commutes in certain days, hence, higher expected EV charge requirements. These differences result in varied demand responses to economic signals, e.g., prices, tariffs, penalties, from each prosumer. However, even if all households are equipped with these smart energy systems and they are aligned with the current energy market congestion may arise, as explored in section 2.2. In the following chapter 4 the case study to benchmark congestion based on the input data of each household is detailed.

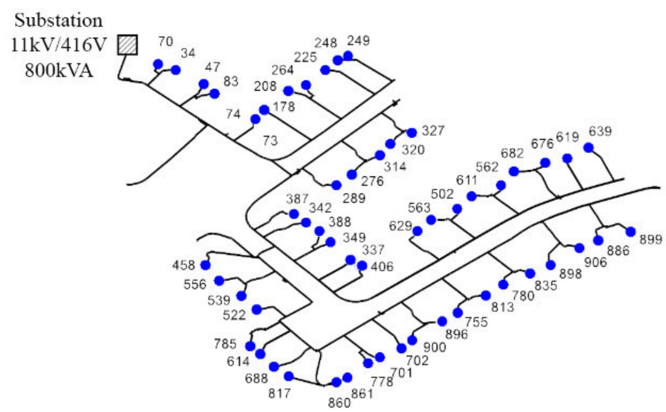

Figure 3.3: Single line diagram of the IEEE European low voltage feeder

4 CASE STUDY AND BENCHMARK FOR CONGESTION IN THE FEEDER

The purpose of this chapter is to describe the case study used to prove that indeed congestion in the feeder will arise in future decentralized energy systems. This is achieved by aligning each of the 55 prosumers in the low voltage feeder to an energy tariff and optimizing their power schedules. This will result in a benchmark to compare and evaluate the market mechanisms investigated in subsequent chapters. First, section 4.1 describes the scenarios used for the case study. Second, section 4.2 elaborates on the assumptions taken in the study. Third, section 4.3 details the input data fed to each of the 55 smart charging algorithms in the network. Fourth, section 4.4 presents the results of the optimized schedules and congestion levels for each scenario.

4.1 SCENARIOS OF THE CASE STUDY

The presence of congestion in the feeder depends heavily in the conditions in which prosumers find themselves in, therefore, it is key to choose scenarios that are representative of these different conditions. Throughout the year prosumers will face a virtually infinite combination of internal and external conditions. For example, load and heat demands due to individual preferences and weather, different levels of irradiance with different sets of PV installed capacities, EV requirements, and energy prices subject to weather, infrastructure and market dynamics. Nevertheless, on the yearly aggregate trends tend to be fairly stable with few extreme cases.

The approach for this case study was to select two extreme scenarios where prosumers would have to optimize their power schedules, and evaluate the response of each prosumer and congestion in the feeder. The assumption is that by optimizing in the extreme cases the problems that may arise in less extreme cases will also be implicitly solvable. The two scenarios are: 1) an extremely cold winter day, and 2) an extremely high irradiance summer day.

1. **Winter scenario** Cold winter day with highest heating demand coupled, with general scarce generation at a transmission level resulting on high energy prices.
2. **Summer scenario** Sunny summer day with the highest irradiance and low load demand, coupled with general abundant generation at a transmission level resulting on low energy prices.

4.2 ASSUMPTIONS AND CONSIDERATIONS

On top of the scenarios there are several general assumptions and considerations in the case study. These are the following:

- **Loads:** Each of the 55 households has its own load profile, which represents the AC appliances without heating.
- **Heating:** The 55 households are divided into 5 tiers (11 households in each tier). These 5 tiers are used for the heating profiles, which increase their peak demands in 5 steps.
- **PV:** The same 5 tiers are used for PV installed capacity assuming that the higher the heat demand, the bigger the household volume, and the larger roof area for installation. The PV installed capacity range is [2kW$_p$ - 10kW$_p$] with a linear increase of 2kW$_p$.
- **Energy storage degradation:** Both BES and EV are composed of the same NMC cells, meaning, subject to the same aging and degradation costs, as per equations .3 and 3.5.
- **BES:** Each household has the same new BES with maximum charge/discharge 10kW capacity and an energy capacity of 10kWh. The state of charge of the battery is limited to between 10% and 90%.
- **EV:** All household have one EV with a 10kW charge/discharge capacity and 80 kWh of energy capacity. The EVs' scheduled commutes are predefined based on the time of departure t_{depart} and arrival $t_{arrival}$; during this time the EV is unavailable (unconnected to the multi-port). The user can choose the minimum state of charge required at t_{depart}. For the commute an efficiency of 15kWh / 100km and an average single trip of 30km are assumed [13]. When the EV returns the state of charge is updated.
- **Demand elasticity:** The appliances' loads and heating (both AC) are non controllable, thus, they need to be supplied without the possibility of shedding. The controllable side consists of the BES, EV and PV power; these are control variables in the smart charging algorithm.
- **Optimization:** All households are equipped with the same smart charging algorithm for cost minimization. The same economic signals apply to all households, i.e., prices, tariffs and penalties. The combination of profiles is assigned randomly to all households, except for PV capacity and heating peak demands, as explained above.

4.3 INPUT DATA

Having laid the scenarios and assumptions, the input data is detailed in this section. The data consists of two sets for each of the parameters, the forecast is in a 15min resolution and the actual data in a 1min resolution. The data profiles are obtained from various real-life sources as explained below.

4.3.1 PV data

The source of the PV data is a single profile of actual data. The forecast profile was generated by averaging the actual profile every 15 min time steps and multiplying the averages with a randomized vector between [0.9 1.15] for every household. This procedure yields forecasts that do not have the same average as the actual data, even if both the actual and forecast profiles come from the same source data. Figure 4.1 shows the forecasted power generation for each of the 5 tiers in the two scenarios. Figure 4.2 compares the actual and forecasted power generation of a single household.

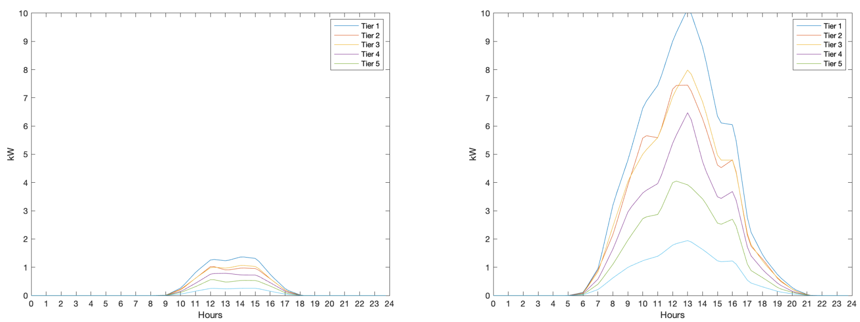

(a) Winter scenario

(b) Summer scenario

Figure 4.1: PV generation forecast of each tier

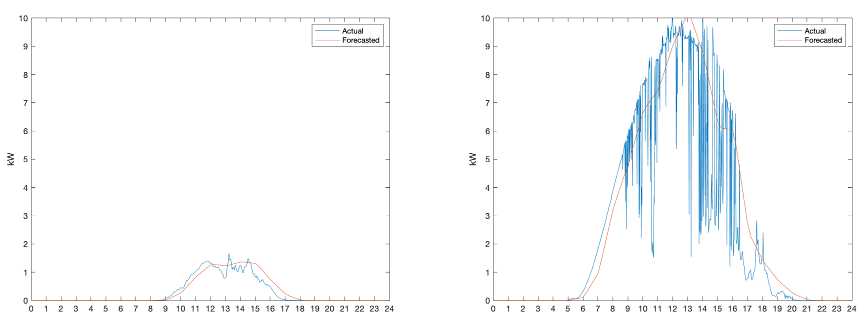

(a) Winter scenario

(b) Summer scenario

Figure 4.2: Actual and forecast PV profiles of tier 1

4.3.2 Load data

The actual load profiles are sourced from the Dutch DSO Alliander, this data was measured from 77 residential clients in 2018. To arrive at 55 profiles, the clients with highest peak power [W] and highest energy consumption [Wh] were selected. The forecasted data is the average load profile from all types of buildings, and then randomized for the 55 households with the same treatment as the PV data above. The rationale is that, in general, loads are highly stochastic and the forecasts are aggregated trends. In figure 4.3 5 forecasts profiles or each tier and scenario are presented. In figure 4.4 a comparison between actual and forecasted profiles is found.

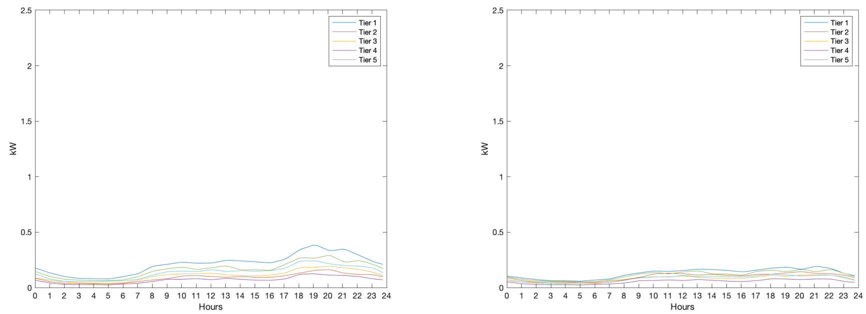

(a) Winter scenario (b) Summer scenario

Figure 4.3: Load forecast of each tier

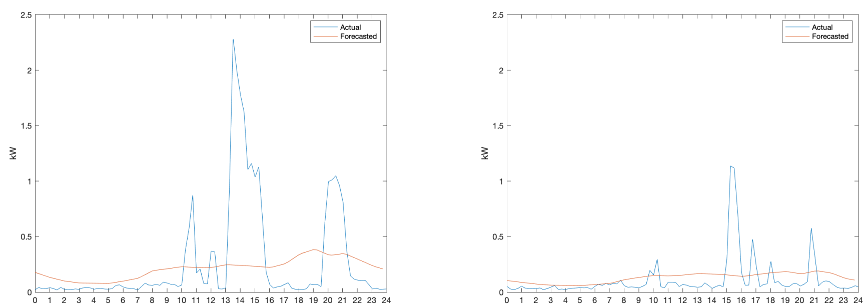

(a) Winter scenario (b) Summer scenario

Figure 4.4: Actual and forecast load profiles of tier 1

4.3.3 Heating data

The heating profiles come from the measurements of electric heat pumps done by TNO in 2015 [54]. These are 5 distinct profiles that are assigned to each of household depending on the tier they belong. The forecasted data is an average for the month of January (winter scenario) and August (summer scenario). The actual data is the profile of the highest demand day and the highest irradiance day of the year, and then randomized with the same [0.9 1.15] vector as above. Figure 4.5 and 4.6 illustrate the profiles for each tier in each scenario, and actual and forecasted profiles, respectively.

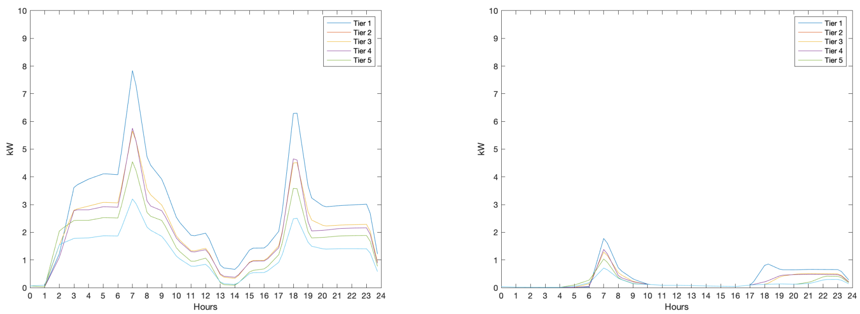

(a) Winter scenario **(b)** Summer scenario

Figure 4.5: Heating forecast of each tier

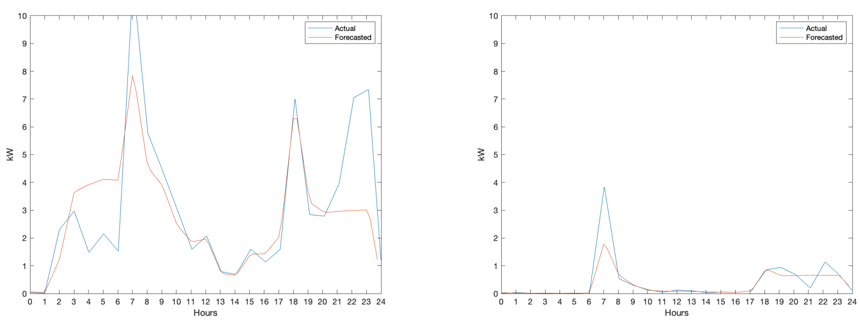

(a) Winter scenario **(b)** Summer scenario

Figure 4.6: Actual and forecast heating profiles of tier 1

4.3.4 EV data

The EV schedules of each household are taken from Alliander's data on charging stations. This data is divided into public and private spaces for weekdays and weekends. With this data a distribution of 55 schedules is constructed and assigned to each household. This means that each of the 55 households has its own unavailability where the EV is disconnected from the multi-port connection and cannot be considered in the optimization for those hours. The range of the unavailable hours is [0h-10h] and has an average of 8.4h. Both scenarios have the same EV schedules, figure 4.7 shows the EVs' distribution of (un)availability.

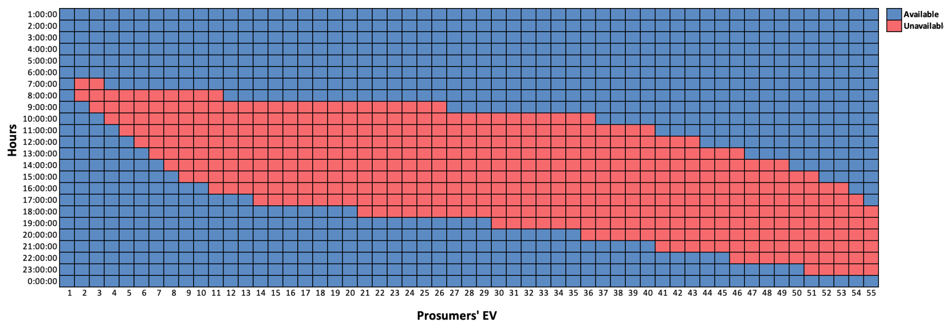

Figure 4.7: Availability distribution of EVs

4.3.5 Price data

In order to obtain the benchmark for congestion the price signals considered are energy tariffs for buying and selling frequency. The price in the energy market is equal to the Amsterdam Power Exchange market (APX) in 2018 [4] averaged to 0.20 €/kWh. As mentioned in section 3.7, the average selling price is 50% lower than the buying price. Figure 4.8 presents the prices for both scenarios. It can be observed that these prices represent extreme cases, especially in the summer scenario where prices go to negative between 14:00h and 16:00h, presumably, due to generation abundance.

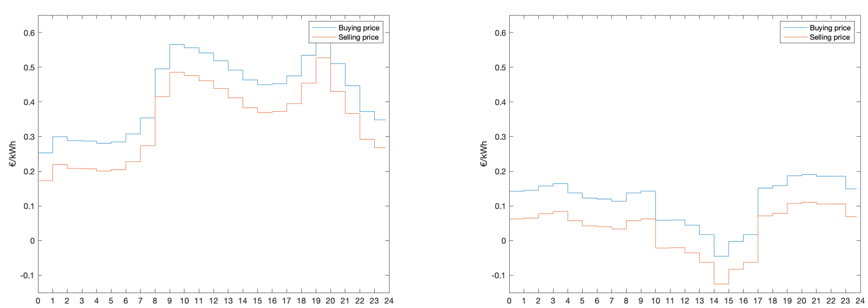

(a) Winter scenario

(b) Summer scenario

Figure 4.8: Energy and regulation prices for each scenario

4.4 RESULTS AND BENCHMARK

4.4.1 Optimized power flows

The optimized power schedules of the 55 prosumers are the result of considering all the assumptions and feeding the input data presented into the smart charging algorithm. The power flows of the components of two different households reacting to price are presented in figures 4.9-4.10 for both scenarios. Figure 4.9 is household No. 1 from EV schedules 4.7, and has the EV available the whole day. Notice that P_{EV} is active throughout the day with high drawing and feeding peaks. Figure 4.10 is a common case where the EV is unavaiable from 9:00 to 18:00 and cannot provide storing flexibility, it is household No. 24.

It is worth mentioning that positive values for P_{Grid} mean feeding the grid (and negative drawing), for P_{BES} and P_{EV} positive charges (and negative discharges); this sign convention will be maintain in the whole thesis. From the figures it is clear that the smart charging algorithm is working in the desirable way. For example, in the winter case high load and heating demand with high prices are exhibited, therefore the stored energy is used as much as possible to avoid exposure to high prices and reduce P_{Grid} In summer, when prices are negative big drawing peaks to store energy and feed back in the evening with higher prices.

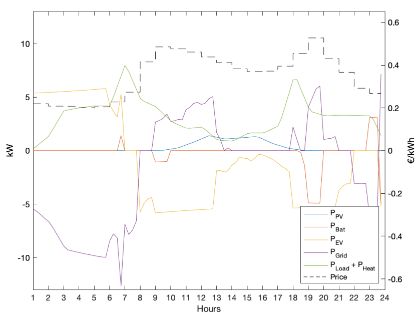

(a) Winter scenario

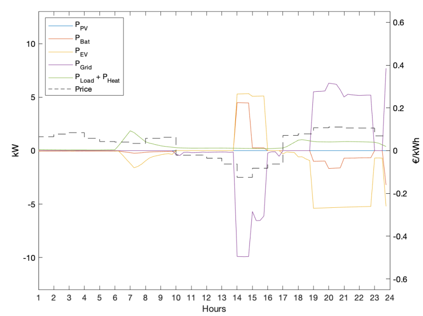

(b) Summer scenario

Figure 4.9: Optimized power flows of household 1 (EV available 24hrs)

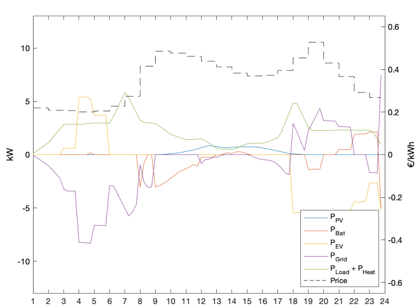

(a) Winter scenario

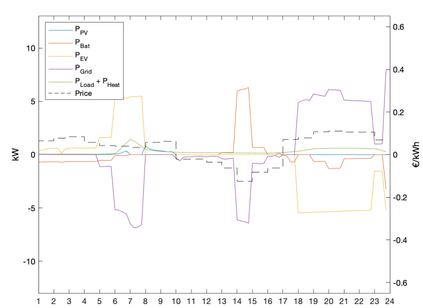

(b) Summer scenario

Figure 4.10: Optimized power flows of household 24 (EV available 14hrs)

4.4.2 Grid exchange

From the feeder's standpoint, the only important profile is the power exchange with the grid because this will determine congestion in it. The grid exchange profiles from the 55 households in the feeder are presented in figure 4.11. Expectedly, a general pattern can be observed from all the profiles because all are residential prosumers and they are responding to the same price signals with the same optimization scheme. Even though, they have different needs and preferences that result in the variations also seen in the figures.

The winter case shows a big demand in the first hours of the day. This may be explained due to very cold weather with high heating demands, but more interestingly, the expectation of a rise in energy prices induces an over consumption for storage and later selling. The PV generation, although small, does provide some relief to grid drawing for the hours it is available.

The summer case illustrates a more extreme situation where, even if there is a high irradiance, no power is been fed back until later in the day where the prices are more attractive. Unsurprisingly, power is been drawn at nearly the power rating of the inverter (10kW) when the prices are negative. These negative prices mean that prosumers are been paid to draw from the grid and charged for feeding in, which indicates high generation abundance. This is quite a drastic situation, nevertheless it is inline with the extreme scenarios described in section 4.1. Notably, for several hours at the beginning of the day and between 8:00h and 10:00h no grid change at all is required because the storage can supply the small loads.

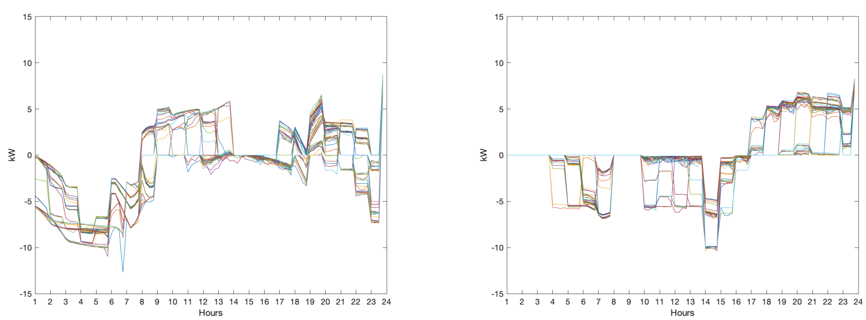

(a) Winter scenario **(b)** Summer scenario

Figure 4.11: Grid power exchange from 55 households in the feeder (+ feeds, - draws)

4.4.3 Congestion in the feeder

It is key to understand how the grid will be affected in decentralized future energy systems were prosumers have in place smart energy systems similar to the one presented in chapter 3. Modeling the IEEE European low voltage test feeder with the optimized power schedules of the prosumers gives a picture of the potential behavior of the distribution network. Figures 4.12-4.13 show this behavior in the two scenarios compared to the standard IEEE loads. These figures are for BUS 1 at the beginning of the feeder, and BUS 906 at the end of it. From figure 4.12a and 4.13a it can be observed that at BUS 1 there is a small deviation in the voltage, however, in figures 4.12b and 4.13b for BUS 906 the voltage has surpassed by a big margin the operational limits of [0.9 1.1] pu. These violations coincide with the big overlapping power peaks due to the price signals, as observed in figures 4.11a and 4.11b.

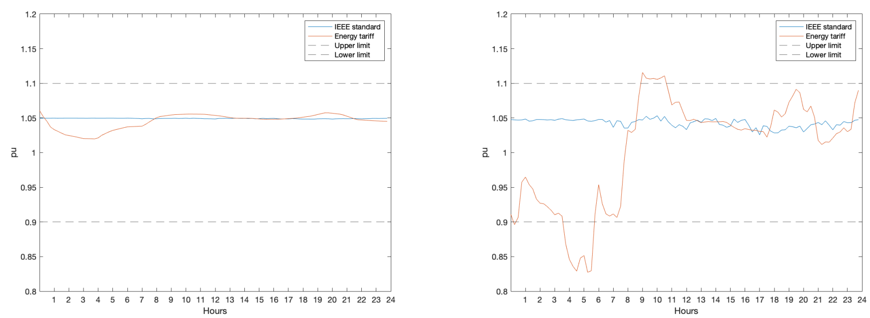

(a) Voltage BUS 1 **(b)** Voltage BUS 906

Figure 4.12: Voltage in the feeder in winter scenario

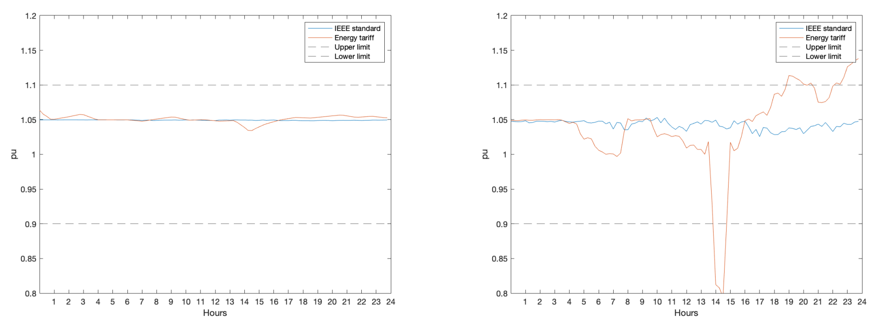

(a) Voltage BUS 1 **(b)** Voltage BUS 906

Figure 4.13: Voltage in the feeder in summer scenario

The energy tariff is the clearing price where wholesale demand and supply are matched. For example, in the summer scenario energy prices drop to even negative values around noon (highest PV irradiance) because the system is flooded with generation and there is not enough demand for it. At a wholesale level the system is signaling that there is an abundance of generation (hence the low price), however, at a distribution level this causes great congestion problems because almost every household is drawing at maximum storing power to sell later.

This illustrates how energy tariffs are inefficient at assigning value to available capacity and flexibility at a distribution level, as reviewed in 2.2.2. These results support the general discussion reviewed in chapter 2, that calls for new market mechanisms that can address demand response and flexibility at a distribution level. Therefore, the congestion levels obtained from the grid model by optimizing the power flows of each prosumer will be the benchmark for the market mechanisms analyzed in chapters 5-7.

5 EVALUATION OF CAPACITY MECHANISMS

This chapter contains the evaluation of four capacity mechanisms whose purpose is congestion management through prosumers' demand response. The selection of the mechanisms is based on the discussion in section 2.2. The mechanisms are: 1) a hard constraint (as a generalization of physically limiting load techniques), 2) capacity subscription, 3) peak tariff, and 4) dynamic tariff. The chapter is consists of 3 sections. In section 5.1 a description of each mechanisms with its mathematical formulation is detailed. In section 5.2 the determination of the key parameters of each mechanism is explained. In section 5.3 the results and analysis of the mechanisms are discussed.

5.1 DESCRIPTION AND FORMULATION OF THE MECHANISMS

The straightforward method to mitigate congestion is to physically limit the peak power from prosumers whenever congestion is present or expected, however, this does not provide prosumers with a choice. This diverges from the paradigm of a liberalized decentralized energy market because it discards any assignation of value to prosumers' flexibility. Nevertheless, it is useful to compare it against market based mechanisms for a more robust analysis. The formulation of a these mechanisms consist on modifying the grid's cost minimization function 3.7 (as presented in the sections below). It is worth mentioning that regardless of the mechanism in place, prosumers are limited by their physical connection to the grid $P_{Grid}^{Max} = 17.5$ kW.

5.1.1 Hard constraint

There are several techniques for congestion management based on direct physical measures, e.g., active power curtailment, automated demand response, and graceful degradation. Here, a hard constraint is used as a generalization of the various techniques. A hard constraint simply means physically limiting the load after a certain power threshold Π_{Sub}. The assumption is that the determination of the threshold will depend on the DSO and the prosumers will know such limit. Then, equation 3.7 becomes 5.1 in the optimization problem. It is relevant to point out that $|P_{Grid}^{Buy}(t)$ and $|P_{Grid}^{Sell}(t)$ are never simultaneously non-zero, as discussed in 3.2.

$$\begin{aligned} C_{Grid}^{Hard} &= \sum_{t=1}^{T} P_{Grid}^{Buy}(t)\lambda_{Buy}(t)\Delta t - \sum_{t=1}^{T} P_{Grid}^{Sell}(t)\lambda_{Sell}(t)\Delta t \qquad \forall t \\ \text{s.t.} \quad & |P_{Grid}^{Sell}(t) - P_{Grid}^{Buy}(t)| \leq \Pi_{Sub} \end{aligned} \tag{5.1}$$

5.1.2 Capacity subscription

The approach for the capacity subscription is based on [3] and [7]. It takes a similar approach to the hard constraint where a power threshold Π_{Sub} is used. In this case, the threshold is a for the prosumer to determine by subscribing to it. The prosumer pays for the assurance that below that power level the energy tariff paid will be low. After such level the prosumer is exposed to very high penalties $\lambda_{Penalty}$, several times the energy tariff price under the subscription. The prosumer could chose and pay for their subscription level on a yearly, seasonally or monthly basis. Retailer providers seem the most adequate party to provide intel services to prosumers since they would compete by providing more accurate subscription levels tailored to their needs, much like data providers in Telecom.

The optimization problem for grid costs becomes 5.2 - 5.4. Note that the subscription level Π_{Sub} in 5.2 and 5.3 is not a decision variable in the optimization problem, it is a parameter that constraints the problem but unlike the previous case it is not a hard constraint. This means that the prosumer could still surpass the limit and pay the penalty $\lambda_{Penalty}(t)$ for it. This gives flexibility to the prosumer but a very high cost that does not necessarily represent the actual cost of congestion at that instance; the prosumer is penalized regardless if there is congestion or not.

The formulation of 5.2 and 5.3 makes the function continuous by avoiding discretization with conditional logic $if\ P_{Grid}^{Buy/Sell}(t) > \Pi_{Sub}$ for penalty payments. Since $P_{Grid}^{Buy/Sell}(t)$ is always positive, the difference $P_{Grid}^{Buy/Sell}(t) - \Pi_{Sub}$ will be negative when $P_{Grid}^{Buy/Sell}(t) < \Pi_{Sub}$ and will be canceled with $|P_{Grid}^{Buy}(t) - \Pi_{Sub}|$. When $P_{Grid}^{Buy/Sell}(t) > \Pi_{Sub}$ both differences (with and without absolute operator) will be positive and doubled, hence, the division by 2. In general, continuous functions are more desirable than discrete ones in optimization problems because they reduce computation expense, therefore this same formulation will be used in for penalty payments in the mechanisms below.

$$C_{Sub}^{Buy} = \sum_{t=1}^{T} P_{Grid}^{Buy}(t)\lambda_{Buy}(t)\Delta t + \frac{P_{Grid}^{Buy}(t) - \Pi_{Sub} + |P_{Grid}^{Buy}(t) - \Pi_{Sub}|}{2}\lambda_{Penalty}(t)\Delta t \tag{5.2}$$

$$C_{Sub}^{Sell} = \sum_{t=1}^{T} P_{Grid}^{Sell}(t)\lambda_{Sell}(t)\Delta t - \frac{P_{Grid}^{Sell}(t) - \Pi_{Sub} + |P_{Grid}^{Sell}(t) - \Pi_{Sub}|}{2}\lambda_{Penalty}(t)\Delta t \tag{5.3}$$

$$C_{Sub}^{Grid} = C_{Sub}^{Buy} - C_{Sub}^{Sell} \tag{5.4}$$

5.1.3 Peak tariff

This mechanism elaborates on the work of [44]. The peak tariff further develops on the idea of providing prosumers with a more active role on the market. In the present case, a tariff φ_{Peak}^{Buy} and φ_{Peak}^{Sell} is paid for the peak power achieved for drawing P_{Peak}^{Buy} and feeding P_{Peak}^{Sell}, respectively. This allows for a symmetric capacity mechanism ($\varphi_{Peak}^{Buy} = \varphi_{Peak}^{Sell}$) or an asymmetric one ($\varphi_{Peak}^{Buy} \neq \varphi_{Peak}^{Sell}$). The assumption here is that the prosumer knows in advance, i.e., day ahead, the price of the tariffs and can optimize accordingly. Similar to the capacity subscription, the prosumer gets energy tariffs below the peaks and is exposed to a penalty above them. The optimization problem for grid costs is now equations 5.5 - 5.7.

It is important to remark that now the peak powers $P_{Peak}^{Buy/Sell}$ are decision variables in the optimization problem. Consequently, prosumers are given the flexibility to choose what value they place on power availability. For example, one might have a long commute on the next day and require a full EV charge early in the morning that requires a higher peak than someone with a shorter commute. Prosumers are still subject to an energy tariff which means that their demand response is incentivized by the capacity tariffs $\varphi_{Peak}^{Buy/Sell}$ and energy tariffs $\lambda_{Buy/sell}(t)$. Of course, the relation between these tariffs will impact the output of each optimization, this is discussed in 5.2.

$$C_{Peak}^{Buy} = P_{Peak}^{Buy}\varphi_{Peak}^{Buy} + \sum_{t=1}^{T} P_{Grid}^{Buy}(t)\lambda_{Buy}(t)\Delta t + \frac{P_{Grid}^{Buy}(t) - P_{Peak}^{Buy} + |P_{Grid}^{Buy}(t) - P_{Peak}^{Buy}|}{2}\lambda_{Penalty}(t)\Delta t \tag{5.5}$$

$$C_{Peak}^{Sell} = -P_{Peak}^{Sell}\varphi_{Peak}^{Sell} + \sum_{t=1}^{T} P_{Grid}^{Sell}(t)\lambda_{Sell}(t)\Delta t - \frac{P_{Grid}^{Sell}(t) - P_{Peak}^{Sell} + |P_{Grid}^{Sell}(t) - P_{Peak}^{Sell}|}{2}\lambda_{Penalty}(t)\Delta t \tag{5.6}$$

$$C_{Peak}^{Grid} = C_{Peak}^{Buy} - C_{Peak}^{Sell} \tag{5.7}$$

5.1.4 Dynamic tariff

The last mechanism is a dynamic tariff which builds on the peak tariff. This mechanism has a similar formulation as the previous case, but the tariff $\varphi_{Dynamic}^{Buy}(t)$ and $\varphi_{Dynamic}^{Sell}(t)$ are time dependent. The price paid for the peak capacity achieved $P_{Peak}^{Buy/Sell}$ depends on when the peak is achieved. This allows the dynamic tariffs to reflect the grid's situation in a more granular fashion, by assigning a price for capacity at PTU. Similarly, the prosumer is still subject to energy tariffs and penalties above the peak capacities paid for. The formulation for grid costs takes the form of 5.9 - 5.10.

$$C_{Dynamic}^{Buy} = P_{Peak}^{Buy}\varphi_{Dynamic}^{Buy}(t_{Peak}^{Buy}) + \sum_{t=1}^{T} P_{Grid}^{Buy}(t)\lambda_{Buy}(t)\Delta t + \frac{P_{Grid}^{Buy}(t) - P_{Peak}^{Buy} + |P_{Grid}^{Buy}(t) - P_{Peak}^{Buy}|}{2}\lambda_{Penalty}(t)\Delta t \tag{5.8}$$

$$C_{Dynamic}^{Sell} = -P_{Peak}^{Sell}\varphi_{Dynamic}^{Sell}(t_{Peak}^{Sell}) + \sum_{t=1}^{T} P_{Grid}^{Sell}(t)\lambda_{Sell}(t)\Delta t - \frac{P_{Grid}^{Sell}(t) - P_{Peak}^{Sell} + |P_{Grid}^{Sell}(t) - P_{Peak}^{Sell}|}{2}\lambda_{Penalty}(t)\Delta t \tag{5.9}$$

$$C_{Dynamic}^{Grid} = C_{Dynamic}^{Buy} - C_{Dynamic}^{Sell} \tag{5.10}$$

5.2 DETERMINATION OF PARAMETERS

The determination of the different parameters, i.e., Π_{Sub}, $\lambda_{Penalty}$, and $\varphi^{Buy/Sell}_{Peak/Dynamic}$ plays a key role in the performance of the mechanisms formulated. The evaluation of the mechanisms is based on a technical and economic approach. For the technical side the main focus is the effectiveness of mechanisms at managing congestion below the permissible levels. Solving congestion may come at different costs for different mechanisms. For the economic evaluation three metrics are employed: 1) total lost load in the feeder, 2) cost of the lost load, and 3) total cost incurred by prosumers in the feeder. Both the technical and economic metrics are compared against the energy tariff benchmark presented in chapter 4. This entails that all data inputs, parameters, constraints and formulations apply equally in all cases, except for the formulation of equation 3.7, as explained in section 5.1 above.

5.2.1 Determination of hard constraint and subscription, Π_{Sub}

For the hard constraint and capacity subscription Π_{Sub} is determined in the same way using [3] approach. The method consists on assuming a that in a certain amount of instances the grid will be congested. For this case, it is assumed that 5% of the year's PTUs will be congested. Then, by matching the yearly load duration curve of each household in the feeder with that 5%, Π_{Sub} is set for every household. Figure 5.1 illustrates this procedure for one prosumer in each of the five tiers. Figure 5.2 shows where Π_{Sub} is set for all 55 households.

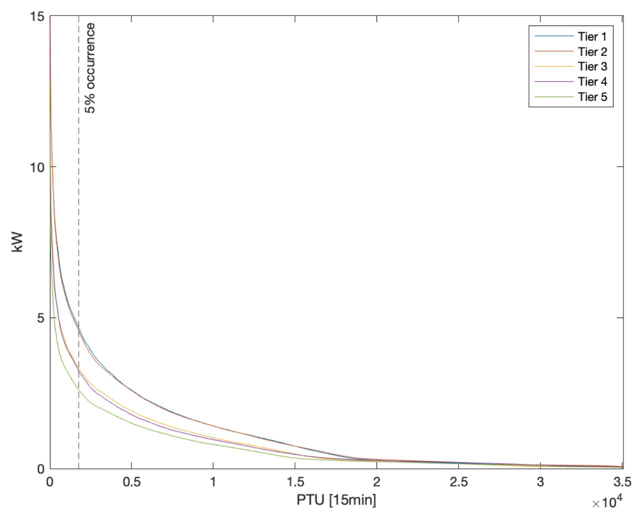

Figure 5.1: Yearly load curve for all tiers

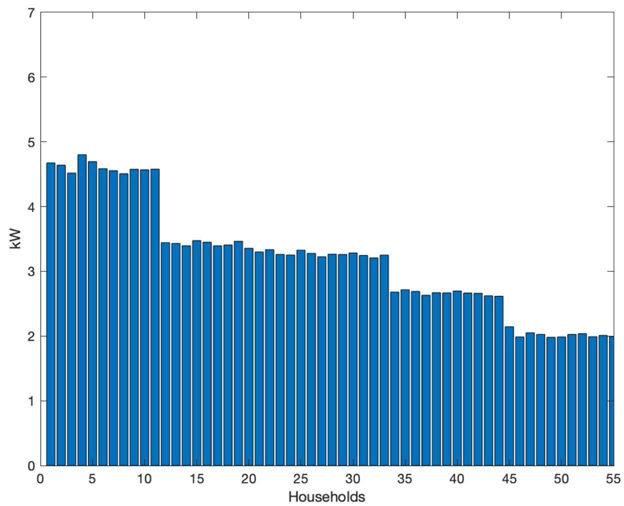

Figure 5.2: Subscribed capacity with 5% congestion occurrence

5.2.2 Determination of peak tariffs, $\varphi_{Peak}^{Buy/Sell}$

The peak tariff $\varphi_{Peak}^{Buy/Sell}$ to feed and draw is determined by analyzing the sensitivity of prosumers different levels of tariffs. A price is set at $\varphi_{Peak}^{Buy/Sell} = 0.015$ €/kW [44] and increased linearly an order of magnitude to $\varphi_{Peak}^{Buy/Sell} = 0.15$ €/kW. Running the simulation for all prosumers a sensitivity curve to price, $\Delta P_{Peak}^{Buy/Sell} / \Delta \varphi_{Peak}^{Buy/Sell}$, can be constructed for all in each scenario. Figures 5.3-5.4 show these curves for drawing and feeding peak capacity in winter and summer, correspondingly. These figures present the peak capacity determined by the optimization as a function of price levels. Figures 5.3a and 5.4a are peak drawing capacities, they never fall to zero because there is load and heating demand (for the most part) that needs to be satisfied. Figures 5.3b and 5.4b are feeding capacities, these do fall to zero at some point because selling energy is not strictly necessary. These peak capacities strongly depend on the energy tariff in place, in this case the summer scenario has lower prices than winter, therefore, the feeding peak capacities fall to zero at lower peak tariff prices compared to the winter scenario.

It is worth noting the somewhat asymptotic nature of the curve, this indicates that after certain price level the smart charging algorithm cannot further reduce the peak capacity because of the inner constraints need to be satisfied, especially in the drawing curve. After this limit any extra increase on the price is punishing prosumers unnecessarily. As a result the tariff is set at $\varphi_{Peak}^{Buy/Sell} = 0.06$ €/kW to allow some room for further increase if needed. Figures 5.5a and 5.5b display the optimized feeding and drawing capacity from each household in the feeder, in each scenario. It can be argued that the proper determination of the tariff should also reflect the cost incurred by the congestion, but such analysis is out of scope of this thesis.

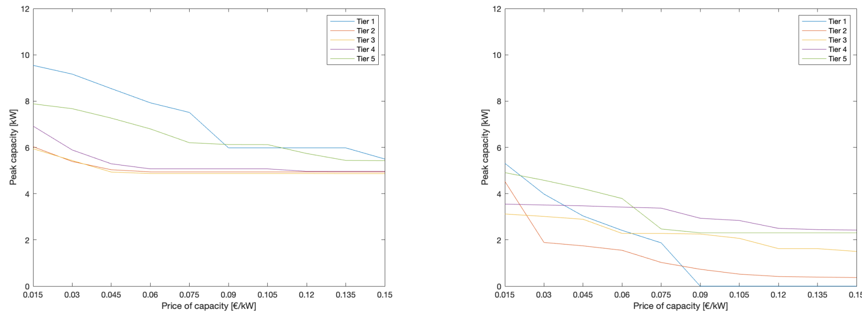

(a) Peak drawing capacity

(b) Peak feeding capacity

Figure 5.3: Price sensitivity of peak capacities for each tier in winter

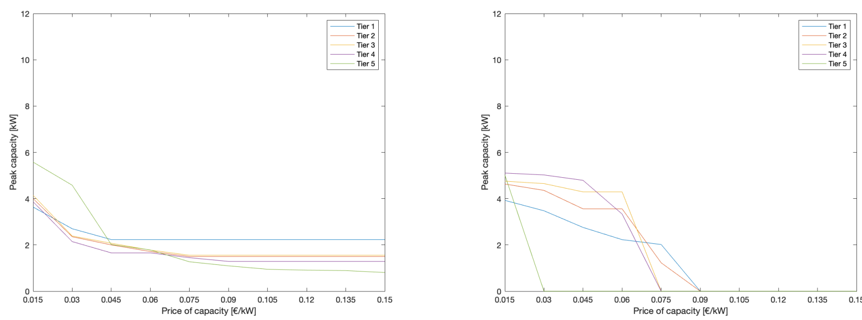

(a) Peak drawing capacity

(b) Peak feeding capacity

Figure 5.4: Price sensitivity of peak capacities for each tier in summer

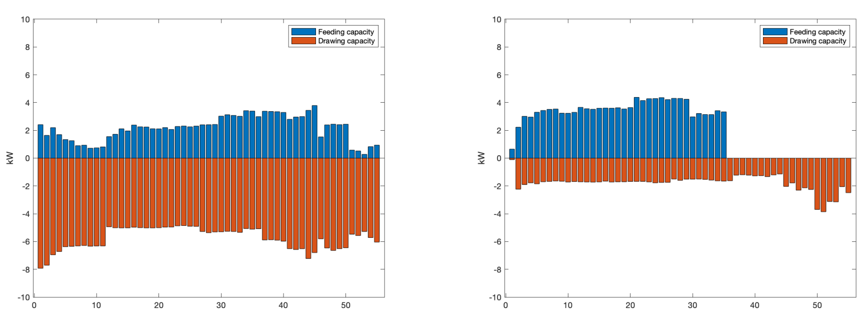

(a) Winter scenario

(b) Summer scenario

Figure 5.5: Optimized peak capacity for each household

5.2.3 Determination of dynamic tariffs, $\varphi^{Buy/Sell}_{Dynamic}$

The determination of $\varphi^{Buy}_{Dynamic}(t)$ and $\varphi^{Sell}_{Dynamic}(t)$ develops on the peak tariff's method. The price sensitivity between [0.015€/kW 0.15€/kW] as presented in figures 5.3 and 5.4 sets the basis for a time dependent version.

In order to reflect the capacity of the feeder as a function of time, the maximum expected congestion from figure 4.12 and 4.13 are matched with the maximum tariff $\varphi^{Max} = 0.15$€/kW. The voltage $v(t)$ deviates from the nominal value $v_{Nom} = 1.0$ pu, then it is divided by the maximum deviation in that time horizon to obtain a [0 1] range. Multiplying times the maximum tariff φ^{Max} yields the maximum price when the maximum deviation occurs. Equation 5.11 shows this calculation. Similar to the peak tariff, this should also include the actual cost of capacity, but is out of scope here.

This procedure is proxy for the competing price signals between energy and capacity. Such competition can be observed in figures 5.6. For instance, the summer case (figure 5.6b) shows a negative energy price between 14:00-15:00hrs implying wholesale generation abundance which signals to draw, at that same instance the tariff is the highest because too much drawing is expected and that would lead to congestion. Notice how the energy and dynamic tariff are not just inversely correlated, by the evening in the summer scenario both rise. In this case, the higher energy tariff from the evening relative to the afternoon is an incentive to feed energy stored earlier, the dynamic tariff responds to that potential feeding congestion too.

$$\varphi^{Buy/Sell}_{Dynamic}(t) = \frac{|v(t) - v_{Nom}|}{max(|v(t) - v_{Nom}|)}\varphi^{Max} \tag{5.11}$$

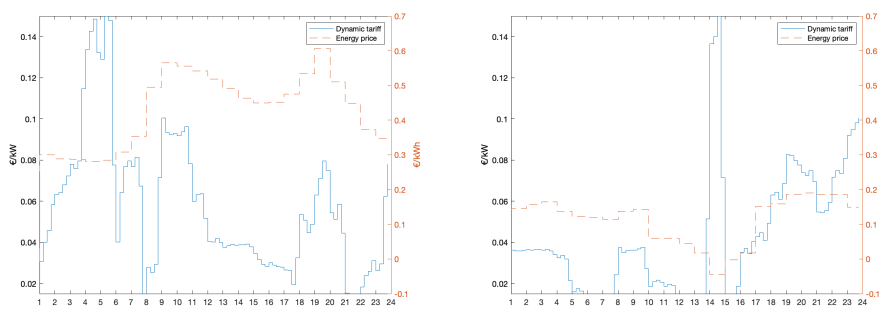

(a) Winter scenario

(b) Summer scenario

Figure 5.6: Dynamic tariff and energy tariff

5.2.4 Determination of penalty, $\lambda_{Penalty}(t)$

The penalty $\lambda_{Penalty}(t)$ is determined with the same approach as the with the peak tariff, by analyzing the sensitivity of prosumers peak capacity to the penalty $\Delta P_{Peak}^{Buy/Sell}/\Delta\lambda_{Penalty}$. The penalty is obtained by multiplying the energy tariff by a factor μ between 5 and 15 [3], as calculated in equation 5.12. Figure 5.7 illustrates the peak capacity achieved by varying the penalty factor. As expected, the penalty level does not make a difference because it is paid only when the peak is surpassed (regardless of mechanism type). Therefore, due to the cost minimization formulation the optimization will always try to avoid incurring any extra costs.

$$\lambda_{Penalty}(t) = |\mu * \lambda_{Buy}(t)| \tag{5.12}$$

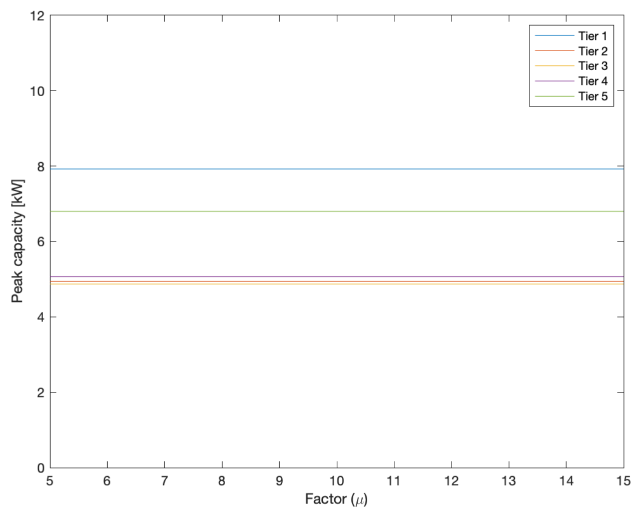

Figure 5.7: Price sensitivity of peak capacities of each tier

5.3 RESULTS AND ANALYSIS

5.3.1 Grid exchange of all mechanisms

The capacity mechanisms implemented as described in sections above yield unique power exchanges with the grid for each household in the feeder. These power exchanges for both scenarios are presented in figures 5.8-5.11. Notably, they all successfully limit drawing and feeding peaks when most needed, i.e., in the first and last hours of the day for the winter scenario, and during the afternoon for the summer scenario. One main distinction between the mechanisms is weather the capacity limits are parameters or decision variables, as stated earlier, for the hard constraint and capacity subscription the limits are parameters, and for the peak and dynamic tariff they are decision variables. The effect of this can be observed in the grid schedules.

For instance, the dynamic and peak tariffs tend to be flatter than the hard constraint and subscription particularly in the summer scenario when load and heating demand are lower. This may be explained because at lower non flexible demands the optimization can spread more evenly, over time, the power drawn (or fed) whenever the capacity limit is a decision variable because minimizing costs implies minimizing capacity prices while satisfying constraints and maximizing selling revenue. Whenever the limits are parameters there is less flexibility to flatten the power drawn/fed because the optimization is constrained by it, meaning that it allocates the grid exchange within does boundaries while trying to avoid penalty costs for the capacity subscription (in the hard constraint it is not possible to surpass them).

Figure 5.12 compares the congestion levels of all mechanisms against the energy tariff benchmark. These results indicate that all mechanisms can be successful at managing congestion for this case study, if properly designed. Furthermore, these results also show that some mechanisms can be more restrictive towards prosumers than others. The key feature of these mechanisms is the determination of the parameters (presented in section5.2) since they dictate the response from prosumers' optimization. For example, the hard constraint is more restrictive than the peak tariff due of to the parameters they operate with. The peak tariff is the closest to the limits of the feeder, however, if a higher tariff is chosen it will restrict prosmuers more, and loosening the limits of the hard constraint and capacity subscription will push closer to the feeder's limits.

In general, the mechanisms make the profiles be less variable in each time step, even for several hours, which is desirable from a congestion management stand point. Of course, this is only possible due to the energy storage of all prosumers, especially for schedules where the EV is available for several hours. For example, household No. 1 where the EV is available during the whole day, as seen inf figure 4.7. However, limiting peaks is not the only desirable feature of the mechanisms. The implications of limiting peaks on overall demand is analysed in the next sections.

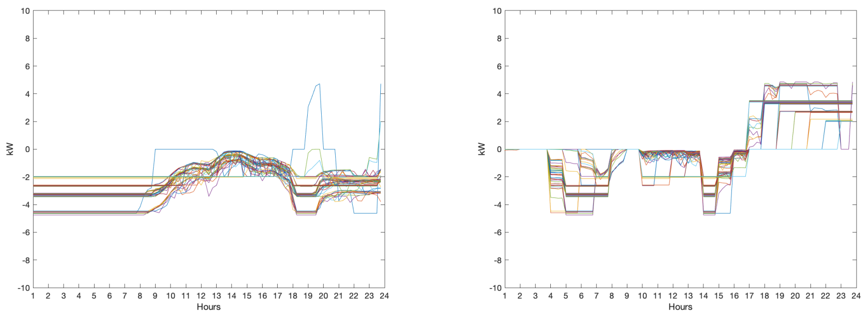

(a) Winter scenario **(b)** Summer scenario

Figure 5.8: Grid exchange of all households with hard constraint

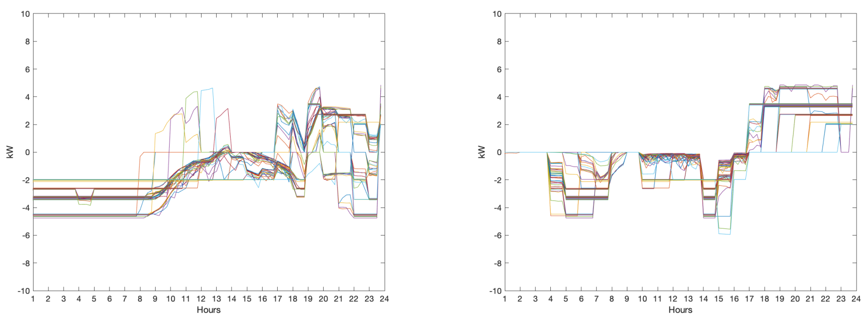

(a) Winter scenario **(b)** Summer scenario

Figure 5.9: Grid exchange of all households with capacity subscription

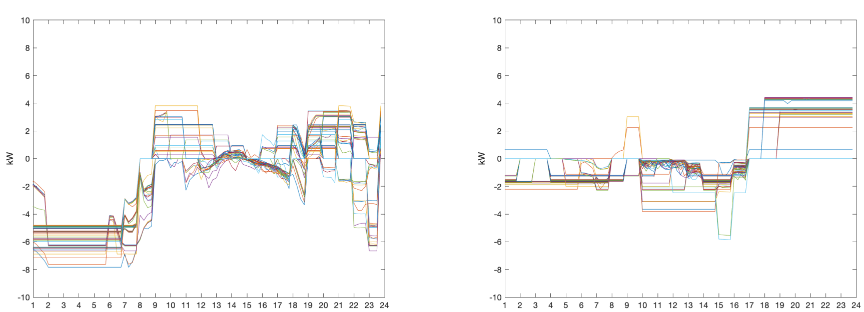

(a) Winter scenario **(b)** Summer scenario

Figure 5.10: Grid exchange of all households with peak tariff

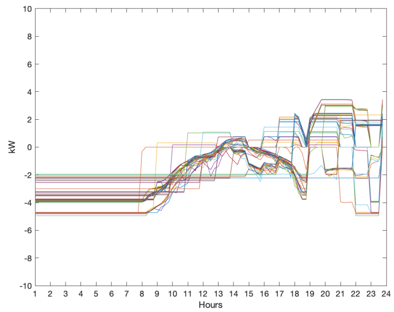

(a) Winter scenario

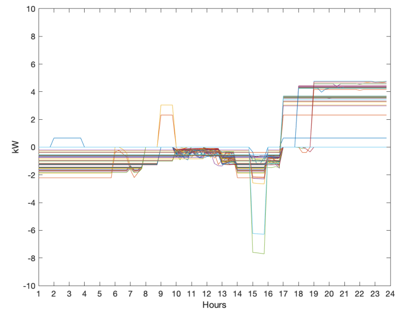

(b) Summer scenario

Figure 5.11: Grid exchange of all households with dynamic tariff

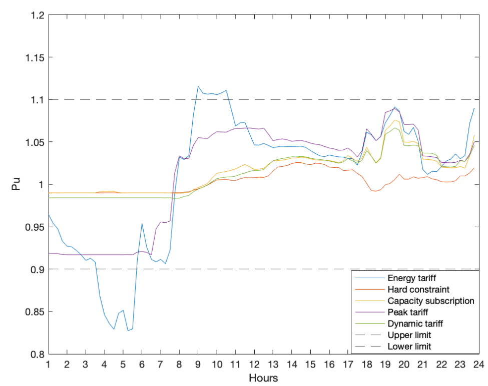

(a) Winter scenario

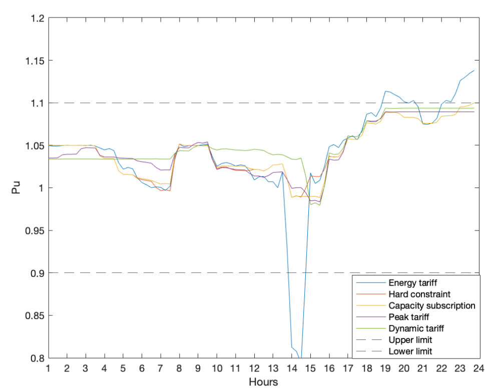

(b) Summer scenario

Figure 5.12: Voltage at BUS 906 in the feeder for all mechanisms

5.3.2 Demand shifted due to mechanisms

It is key to evaluate how much of the demand has been shifted as a consequence of implementing the capacity mechanisms. In order to achieve this, the summation of all household demands in the feeder are benchmarked against the energy tariff only case described in chapter 4. The ideal case would be that the net demand from the energy tariff was kept for all mechanisms, hence, no loss on their utility functions of demand. Figures 5.13-5.12 present the total demand shifted per PTU (15 min). In the figures a negative (-) and a positive (+) value means more demand and less demand, respectively. This, to maintain convention consistency of (-) drawn from the feeder, and (+) fed to the feeder. Generally, it can seen that the winter case for all mechanisms had the biggest demand shifts comparatively to the summer scenario. It is clear that periods of lost demand (+) are compensated to an extent by periods of more demand (-), compared to the energy tariff benchmark. However, not all PTUs weigh the same from a utility point of view, thus, a cost analysis is presented in next section.

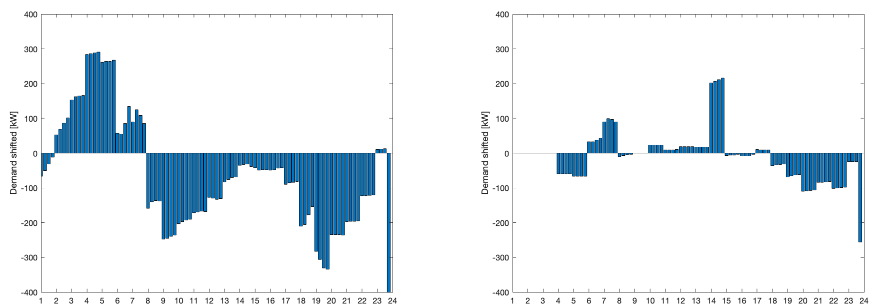

(a) Winter scenario

(b) Summer scenario

Figure 5.13: Demand shifted with hard constraint (- more demand, + less demand)

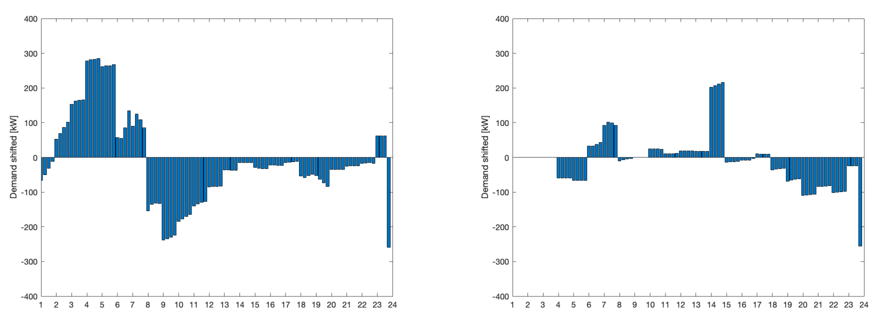

(a) Winter scenario

(b) Summer scenario

Figure 5.14: Demand shifted with capacity subscription (- more demand, + less demand)

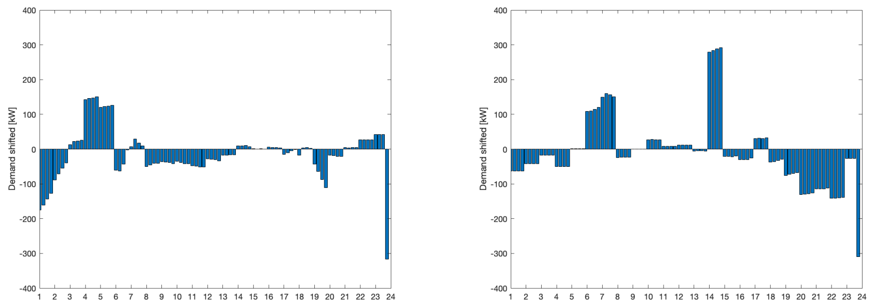

(a) Winter scenario **(b)** Summer scenario

Figure 5.15: Demand shifted with peak tariff (- more demand, + less demand)

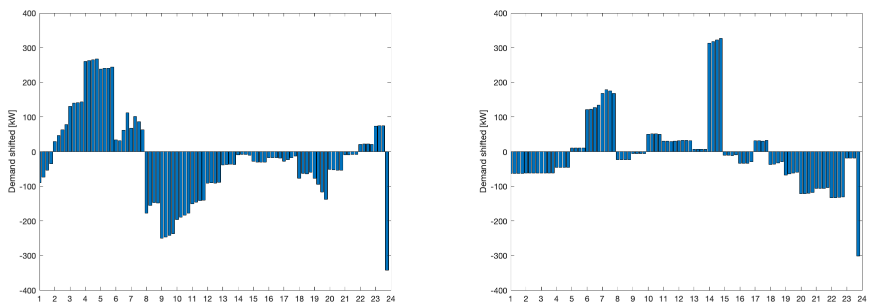

(a) Winter scenario **(b)** Summer scenario

Figure 5.16: Demand shifted with dynamic tariff (- more demand, + less demand)

5.3.3 Cost analysis of the mechanisms

Having presented the technical aspects of the capacity mechanisms in the sections above, an economic analysis is discussed in this section by focusing on three main metrics: 1) Lost load, 2) Cost of lost load, and 3) Total cost incurred by prosumers in the feeder. First, the lost load E_{Lost} is obtained by comparing the summation of all loads of both scenarios in the feeder, for each mechanism against the energy tariff benchmark. Equation 5.13 is used to calculate this. Second, the cost of lost load C_{Lost} is calculated with equation 5.14, assuming that the price $\lambda_{Energy}(t)$ is the market clearing price and reflects the utility of demand at any t. Third, the total cost incurred by the feeder C^{Feeder}_{Total} is the summation of all objective functions (3.1 in the feeder, equation 5.15 is such summation.

$$E_{Lost} = \sum_{h=1}^{H=55houses} \sum_{t=1}^{T=24hrs} E_h^{Energy}(t) - \sum_{h=1}^{H=55houses} \sum_{t=1}^{T=24hrs} E_h^{Mechanism}(t) \tag{5.13}$$

$$C_{Lost} = \sum_{h=1}^{H=55houses} \sum_{t=1}^{T=24hrs} E_h^{Energy}(t)\lambda_{Energy}(t) - \sum_{h=1}^{H=55houses} \sum_{t=1}^{T=24hrs} E_h^{Mechanism}(t)\lambda_{Energy}(t) \tag{5.14}$$

$$C^{Feeder}_{Total} = \sum_{h=1}^{H=55houses} min(C^h_{Total}) \tag{5.15}$$

In figures 5.17, 5.18, 5.19 the lost load, cost of lost load and total cost of all mechanisms are displayed, correspondingly. From the former it can be appreciated that the hard constraint is the mechanisms that loses the most load because it allows the least flexibility to prosumers, whereas the dynamic tariff loses the least. However, analyzing the cost of the load lost it is the peak tariff that shows a better outcome than the dynamic. This may be explained due to the fact that the dynamic tariff prices capacity according to demand size (through expected congestion), thus, it incurs a higher cost to the utility of prosumers. Lastly, the least total cost incurred by prosumers in the feeder is the peak tariff too, therefore, it can be concluded that the peak tariff shows the best performance of all mechanisms for this case study. As a consequence, the following chapters will build their developments on top of the peak tariff.

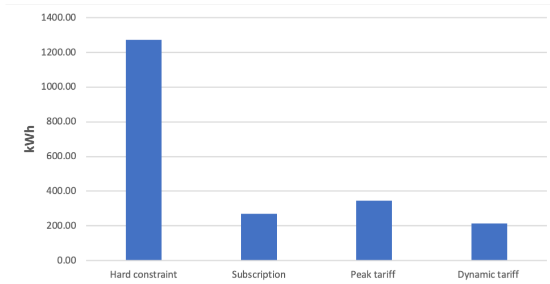

Figure 5.17: Lost load in the feeder

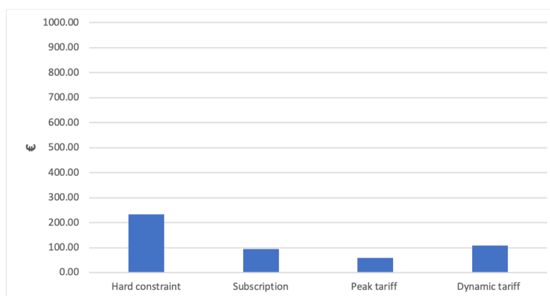

Figure 5.18: Cost of lost load in the feeder

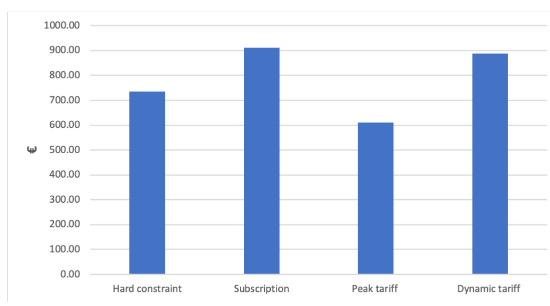

Figure 5.19: Total cost incurred by all households

6 DAY AHEAD AND INTRADAY MARKETS

In chapter 5 the evaluation of four different capacity mechanisms yielded the peak tariff with the best techno-economic performance for the case study. However, in such analysis the effects of forecast errors and imbalance costs were not incorporated. Thus, this chapter describes the integration of a day ahead and intraday market using the Dutch market structure as reference. The goal of this integration is to minimize imbalance costs due to forecast errors by compensating day ahead schedule deviations in the intraday market. Section 6.1 explains the incorporation of said markets with the peak tariff mechanisms. Section 6.2 details the methodology to simulate new forecasts with better accuracy being fed into the smart charging algorithm's moving horizon, and the intraday prices. Section 6.3 presents the results of the simulation and an analysis of them.

6.1 INCORPORATION OF DAY AHEAD AND INTRADAY WITH PEAK TARIFF

In section 2.3 a general overview of the Dutch energy market was presented. The power exchange of the Netherlands operates within the interconnection of Central Western European countries. The venue where most of the short term electricity trading occurs is the EPEX Spot market [12]. In the Dutch day ahead market positions are closed at 12:00hrs one day prior to delivery for the 24hrs of the next day in blocks of 15 min (PTU). This market is an auction where all participants get the same clearing price for every PTU according to where demand meets supply's merit order. Both demand and generation are bids based on expected schedules for the day.

However, real time demand and generation may deviate from the day ahead schedules, in part due to their dependence on forecasts, especially for RES as seen in 2. Thus, the intraday market provides a venue for continuous peer to peer trading to correct the deviations. For the Netherlands, the trading starts at 15:00hrs (three hours after day ahead closure) allowing for trades until 5 min prior to delivery. Since it is peer to peer, there is no single price for any given PTU as discussed in 2.3.2. Further deviations from schedule are subject to the imbalance market where the price paid is typically much higher than previous markets, essentially penalizing for being in imbalance. Figure 6.1 presents the time flow of these markets.

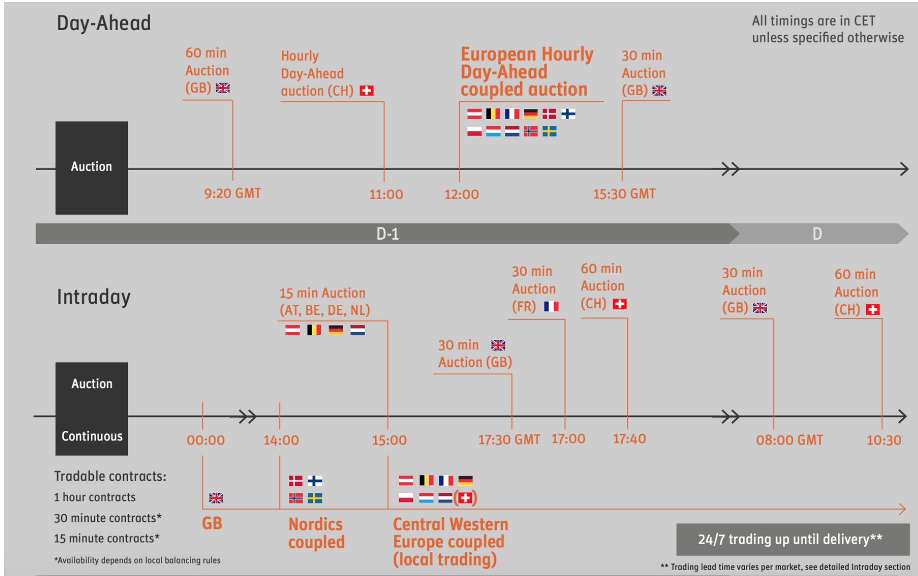

Figure 6.1: EPEX SPOT trading time flow [12]

The integration of these markets with the peak tariff mechanism into the smart charging algorithm has two main objectives: 1) evaluate closer to the real life market dynamics, 2) minimize prosumers' imbalance costs due to deviations caused by forecast errors. In order to achieve these objectives the following assumptions have been made.

Assumptions:

- The day ahead optimized scheduled is determined one PTU before closure, i.e., 11:45hrs, based on the best available forecast at that instance.
- The peak capacity (drawing and feeding) is determined in the day ahead schedule as described in section 5.2.2.
- A new forecast of all data input data 4.3 is used every time step (PTU) with improving accuracy.
- The intraday energy volumes (kWh) for any instance are traded one PTU before delivery, i.e., 15 min prior, at the average intraday price of that time.
- All remaining deviations from the day ahead schedule incur an imbalance penalty.

The costs incurred by the prosumer now also consider equations 6.1-6.4 for the intraday tradings C_{ID} and imbalance costs $C_{Imbalance}$. $P_{ID}(t)$ is the power scheduled one PTU before delivery of t, and $P_{DA}(t)$ is the initial power scheduled day ahead with equation5.7. $P_{ID}^{Sell}(t)$ and $P_{ID}^{Buy}(t)$ are positive and negative, respectively, to maintain sign convention. Figure 6.2 presents the flowchart of the optimization within the different schedules.

$$C_{ID} = \sum_{t=1}^{T} |P_{ID}^{Buy}(t)|\lambda_{ID}(t)\Delta t - \sum_{t=1}^{T} P_{ID}^{Sell}(t)\lambda_{ID}(t)\Delta t \tag{6.1}$$

$$P_{ID}^{Sell}(t) = P_{ID}(t) - P_{DA}(t) \qquad \text{for} \qquad P_{ID}^{Sell}(t) > 0 \tag{6.2}$$

$$P_{ID}^{Buy}(t) = P_{ID}(t) - P_{DA}(t) \qquad \text{for} \qquad P_{ID}^{Buy}(t) < 0 \tag{6.3}$$

$$C_{Imbalance} = \sum_{t=1}^{T} |P_{Actual}(t) - P_{ID}(t)|\lambda_{Imbalance}(t)\Delta t \tag{6.4}$$

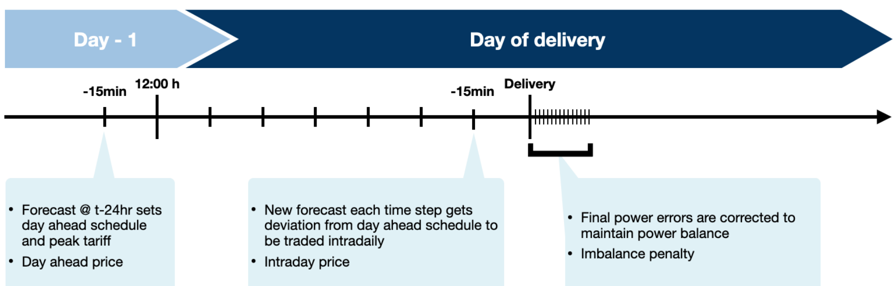

Figure 6.2: Flow chart of optimization with peak tariff, day ahead and intraday

6.2 INPUT DATA AND IMPROVING FORECAST ACCURACY

In order to simulate new forecasts with improving accuracy every time step, new profiles are created based on the same input data described in 6.3c. The assumption is that every time step the forecast will reduce its error from 100% error at $t - 24hrs$ (day ahead) to 5% error at $t - 15min$ (intraday). Figure 6.3 illustrates this simulation for load, heat and PV forecasts. The blue line is the forecast used to optimize the day ahead schedule, it has the highest uncertainty. The yellow line is the actual profile. The orange line shows the simulation of a new forecast received with better accuracy closer to time of delivery.

The simulation initializes at $t = 0$ where the optimization begins with a time horizon of 24 hrs. In the first couple of hours the orange and yellow (simulated and actual) almost overlap but as time horizon becomes larger, the orange line becomes closer to the initial forecast. In practice an actual new forecast would be obtained from various sources and methods, e.g., machine learning, more accurate weather data, etc., however, this approach aims to simulate that behavior. In principle, forecasts would be more accurate closer to the time of realization.

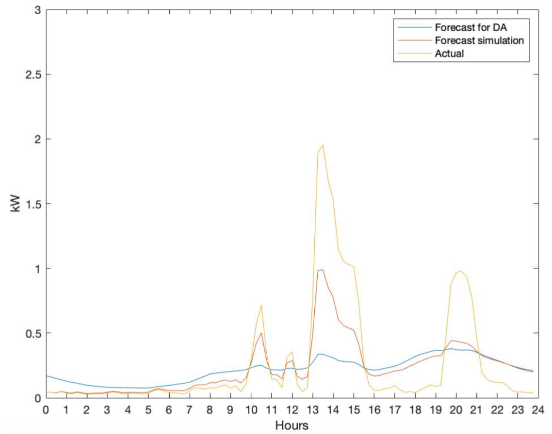

(a) Load forecast

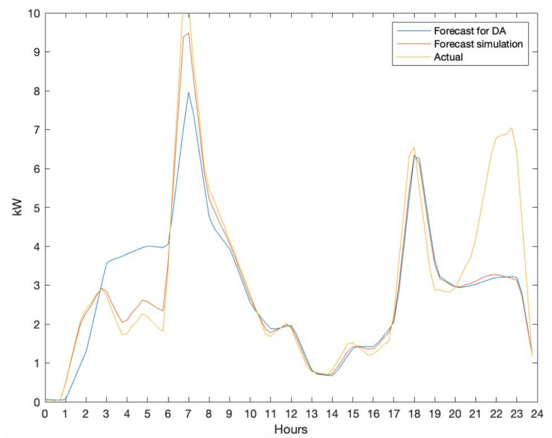

(b) Heat forecast

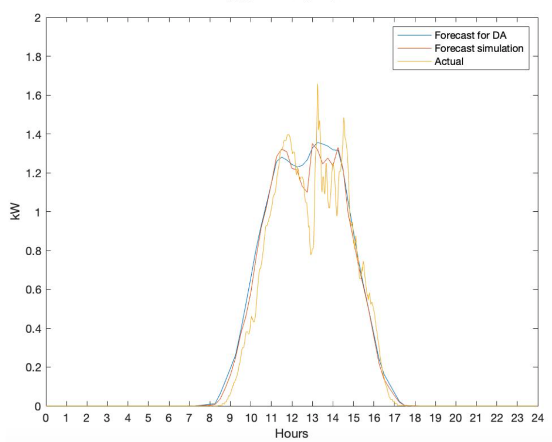

(c) PV forecast

Figure 6.3: Simulation of forecasts improving over time

As mentioned above, there is no single intraday price $\lambda_{ID}(t)$ for every time step as there is for day ahead. Therefore, the profile of $\lambda_{ID}(t)$ is constructed by extracting the actual trading prices λ_{ID}^{Actual} from 2018, and averaging them to the average yearly difference to day ahead prices Δ_{DA-ID}^{Year} reported by Tennet [49] presented in figure 2.7b. Equation 6.5 is the formulation of this procedure, and figure 6.4 compares the results of the formulation with the day ahead price. Lastly, the imbalance penalty $\lambda_{Imbalance}$ is obtained by adding the average imbalance delta of the year $\Delta\lambda_{Imb-DA} =$ 0.0225 €/kWh, reported by TenneT [49], to the day ahead price λ_{DA}. The calculation is done with equation 6.6.

$$\lambda_{ID}(t) = \frac{\lambda_{ID}^{Actual}(t)}{mean[\lambda_{ID}^{Actual}(t)]|_0^T} \Delta\lambda_{DA-ID}^{Year} \tag{6.5}$$

$$\lambda_{Imbalance}(t) = \lambda_{DA}(t) + \Delta\lambda_{Imb-DA} \tag{6.6}$$

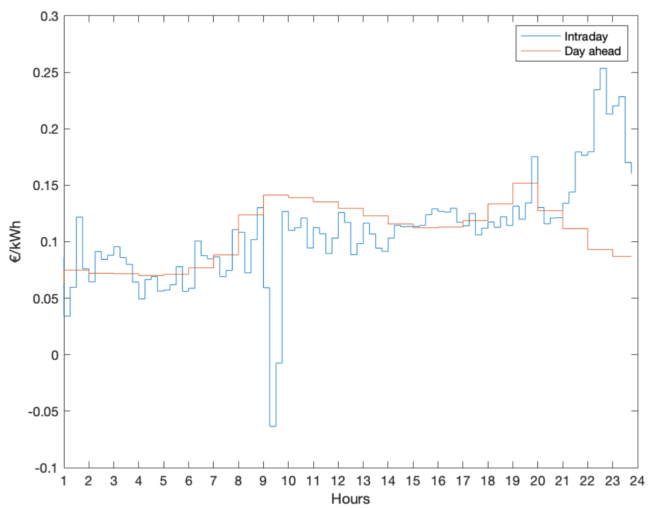

Figure 6.4: Intraday and day ahead prices

6.3 RESULTS AND ANALYSIS

The incorporation of the day ahead and intraday market yields new optimized schedules for grid exchange that try to minimize the exposure to imbalance penalties. The results of this incorporation are presented in figure 6.5 for one household. The day ahead schedule (blue line) is the result of the optimization with the available forecast one day prior to delivery. Then, every time step of the moving horizon (orange line) a new, more accurate, forecast is fed to the smart charging algorithm. The model aims to stay within the initial optimized schedule by adjusting the power flows of the inner components. Whenever it is not possible to stay within the initial schedule, it relies on intraday trades. However, there are still errors due to forecast inaccuracy and difference in time resolution. The forecasted schedules are in blocks of 15 min, and the actual profile in a 1 min basis. This is compensated with the real time control described in section 3.2, hence, the yellow line represents the actual grid exchange.

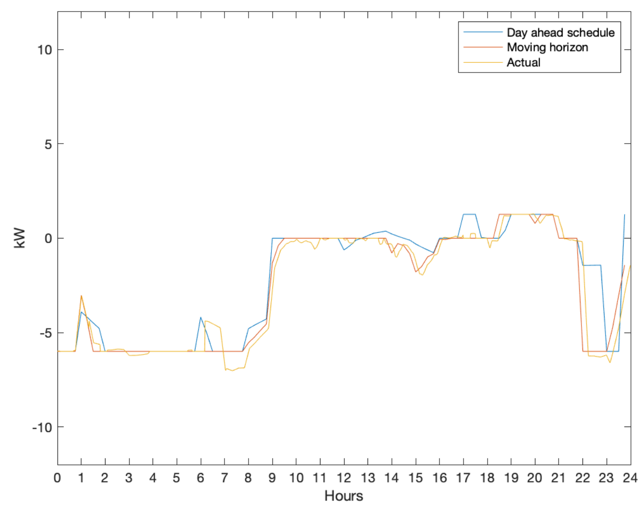

Figure 6.5: Grid exchange from different time frames

Figure 6.6 displays the initial power deviations due to forecast errors, it is the difference between the forecast available for the day ahead optimization and the actual profiles in real time (equation 3.9). Figure 6.7 shows the volumes traded intradaily one time step before delivery, these are the corrections to deviations after new forecasts and adjustments to the power flows of the smart charging algorithm's components. Figure 6.8 presents the remaining errors that are corrected in real time and settled with imbalance penalties. It is worth noting that by including intraday trading in the optimization the power errors are significantly reduced, i.e, from 6.6 to 6.8.

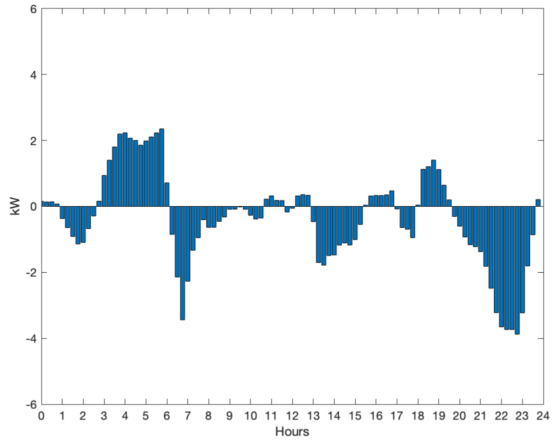

Figure 6.6: Grid power deviations due to forecast errors

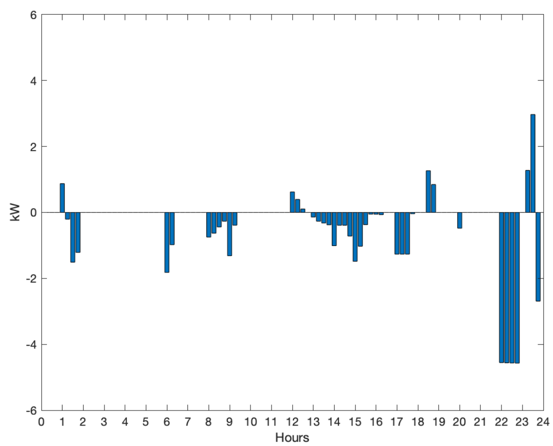

Figure 6.7: Intraday volumes traded

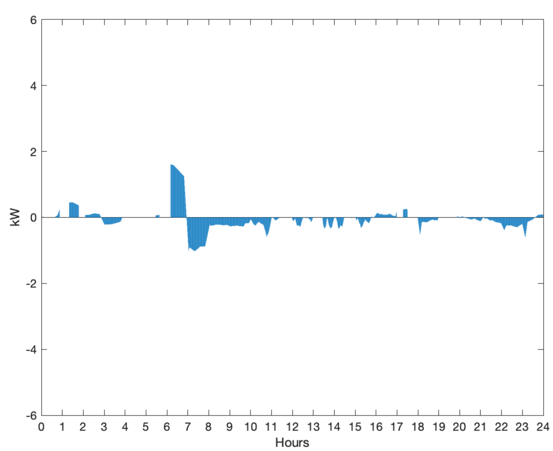

Figure 6.8: Real time corrections with imbalance penalty

Of course, these results depend substantially on the accuracy improvement of forecasts, nevertheless it proves that an integration of current markets with a capacity mechanism can be implemented. Furthermore, it provides relevant insights on the costs reductions that would benefit prosumers. Figure 6.9 presents a cost comparison between having optimized intradaily and not, for the whole feeder. In both cases, the day ahead costs are identical (376.89 €), since the cases were identical thus far. Trading deviations on the intraday adds 304.66 €, and the remaining imbalance cost add to a total of 823.02 €. Whereas not optimizing intradaily adds 567.46 € to the day ahead, with a total of 944.35 €. This provides a combined cost reduction of 13% to prosumers in the feeder, for this case.

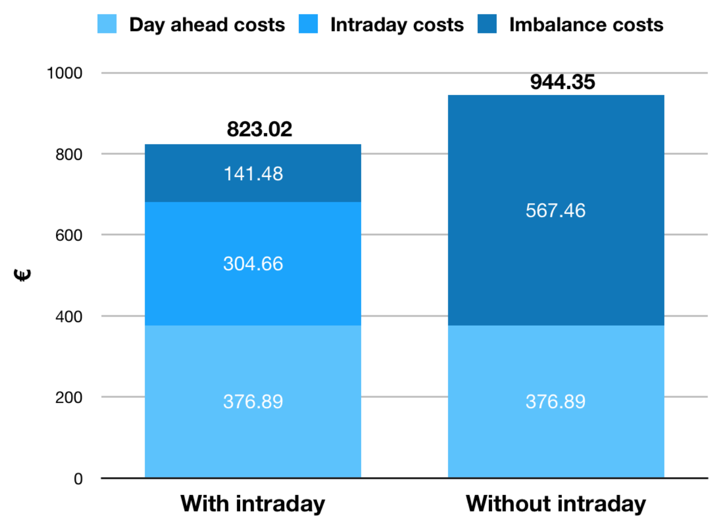

Figure 6.9: Cost comparison with and without intraday optimization

7 FREQUENCY REGULATION AND MARKETS CONFLICTS

The formulation of the smart energy system described in chapter 3 considers the revenue obtained by reserving capacity for primary frequency regulation. Thus far, previous chapter have not considered the implications that providing this power have on the optimized schedules. This chapter incorporates the frequency regulation market, and analyzes the implications on the previous mechanisms studied. Section 7.1 describes the frequency regulation market and the relevance to include it the model. Section 7.2 explains the methodology to determine the power needed for regulation and its effects on power schedules. Section 7.3 presents the results of this incorporation and evaluates the effects on costs, and the compatibility with the capacity mechanism, day ahead and intraday integration.

7.1 DESCRIPTION OF FREQUENCY CONTROL REGULATION

A general overview of the Dutch balance market, frequency containment reserve being part of, is presented in section 2.3.3. The TSO (TenneT) is responsible for maintaining grid's frequency within range of the 50 Hz standard. Whenever there are deviations between scheduled demand and supply there is an imbalance and frequency will deviate form its standard. In order to restore this imbalance, the TSO contracts reserved capacity in an auction through a bidding process. TenneT receives bids from prequalified balancing service providers (BSPs) that want to take part in the auction. BSPs can bid at least 1MW, 14 days prior (D-14) until 1 day prior (D-1) to delivery in 4 hourly blocks [53]. TenneT has recognized the potential of smaller decentralized providers and conducted the *pilot project FCR* to investigate its technical barriers, in the pilot the minimum bid was decreased to 0.1 MW [47].

The TSO decides which bids will be taken based on merit orders for up regulation and down regulation. Upward bids are for feeding power to the grid, and downward bids are for drawing power from the grid. In the Netherlands up and down regulation bids have to be symmetrical, $P_{Bid}^{Up} = P_{Bid}^{Down}$. The up/down power regulation is measured against the latest approved commercial schedule, i.e., feeding more or drawing less than the schedule, up regulates; and feeding less or drawing more, down regulates. On the day of delivery TenneT activates the amount required from the bids to keep grid's stability. Figure 7.1 shows a diagram of the balancing process [51].

7.2 METHODOLOGY

There are to main objectives for incorporating frequency regulation with the previous market mechanisms: 1) to make the smart charging algorithm more versatile to future integrated decentralized energy markets, 2) to evaluate the techno-economic feasibility of such incorporation, at a prosumer and feeder's level. In order to achieve this, the specifications and requirements considered are; maximum insensitivity range, frequency deviation from the standard, and the amount of power that needs to be provided based on the frequency deviation. It is assumed that an aggre-

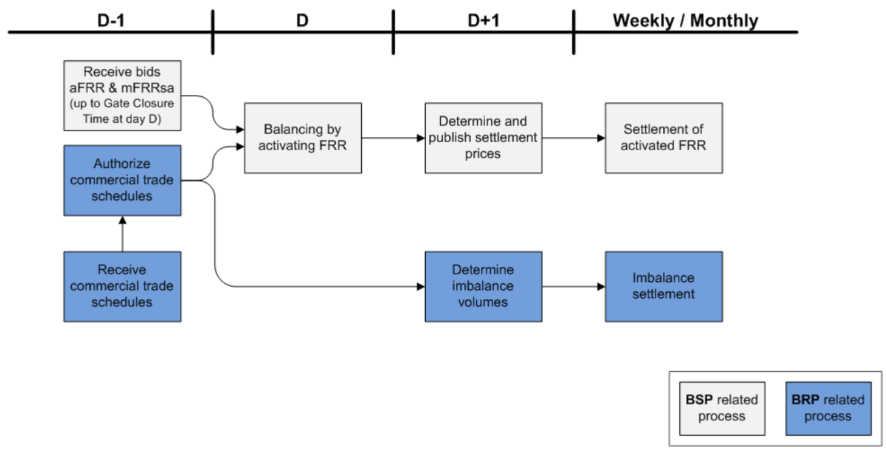

Figure 7.1: Balancing process diagram, [51]

gator will be an intermediary between prosumers and the market to meet minimum capacities and handle all other requirements.

The maximum insensitivity range is 10 mHz, this means that a deviation from the operating point of less than the range does not result in a power change. Any frequency deviation Δf, equation 7.1, from the nominal frequency $f_{nom} = 50$ Hz (above the insensitivity range) requires a power change proportional to the deviation. A deviation of at least ± 200 mHz requires the full capacity reserved. The power required depend on the droop setting of the reserve providing unit (RPU). Equation 7.2 is used to calculate the droop setting. Each unit has its own droop based on their power capacity bid for FCR $P_{Reg}^{Up/down}$ and their nominal power P_{nom} [53]. Consequently, the power needed for regulation from the provider P_{Reg} is determined with equation 7.3.

$$\Delta f = f - f_{nom} \tag{7.1}$$

$$x = \frac{\Delta f / f_{nom}}{P_{Reg}^{Up/down} / P_{nom}} \tag{7.2}$$

$$P_{Reg}^{Actual} = \frac{\Delta f / f_{nom}}{x / P_{nom}} \tag{7.3}$$

The implementation of FCR in the smart charging algorithm was developed by [56], and then adapted for every prosumer in the feeder as described in chapter 3. For this case, the reserve capacity for FCR of each prosumer is constrained by the capacity of the inverter $P_{Inv}^{Max} = 10$ kW, therefore that sets the nominal capacity $P_{nom} = P_{Inv}^{Max}$. Figure 7.2 illustrates the FCR power curve for 5 kW reserved capacity as a function of frequency deviation based on equations 7.2 - 7.3.

It is important to note that FCR participation is added to the peak tariff (it showed the best performance in 5) with the day ahead and intraday markets as described in chapter 6. This means that the smart charging algorithm will determine in the day ahead (D-1): peak capacity $P_{Peak}^{Buy/Sell}$ (equation 5.7), grid exchange $P_{Grid}^{Buy/Sell}$ (equation 3.7), and capacity reserved for frequency regulation $P_{Reg}^{Up/down}$ (equation 3.8).

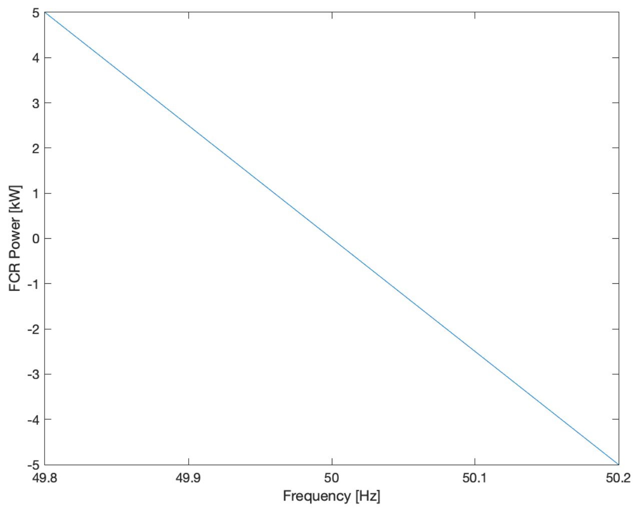

Figure 7.2: Droop corresponding to 5kW reserve capacity and 10kW nominal capacity

Consequently, corrections in the intraday will include deviations due to forecast errors (as before) and also corrections due to power called for regulation. The actual power provided for FCR P_{Reg}^{Actual} (equation 7.3) is not forecasted, thus, it is supplied in real time and updated for the next time step of the moving horizon.

7.3 RESULTS AND ANALYSIS

This section presents the results from the incorporation of FCR as described above, additionally, it analyzes the implications and compatibility of FCR with all market mechanisms involved. Firstly, figures 7.3 and 7.4 present the frequency deviation from the 50 Hz standard, and the power requirement for regulation from one household, respectively. A positive value value in figure 7.3 (according to equation 7.1) means that frequency is above the standard and power needs to be drawn from the grid. This results in a negative value in figure 7.4 maintaining sign convention, and vice versa. It can be noted that around 5:00 hrs and 23:59 hrs the deviation is close to +100 mHz, half the requirement for maximum capacity of +200 mHz. As a consequence the power supplied is around 5 kW, half the reserved capacity at that instance. Lastly, figure 7.5 displays the grid exchange from the different optimized schedules. The day ahead is the schedule set at 11:45 hrs one day prior with the best available forecasts, the moving horizon is the schedule with the intraday corrections one time step before delivery (t-15min), and the actual profile with FCR is the actual exchange with the grid considering remaining forecast errors and power for regulation.

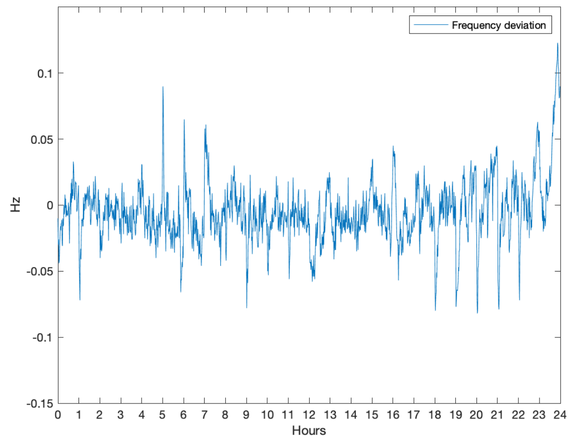

Figure 7.3: Frequency deviation

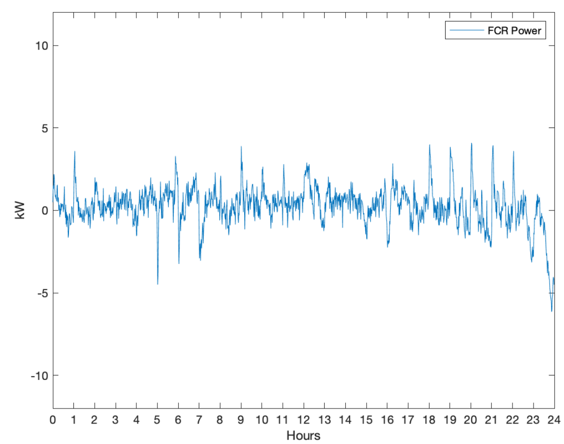

Figure 7.4: Power called for regulation

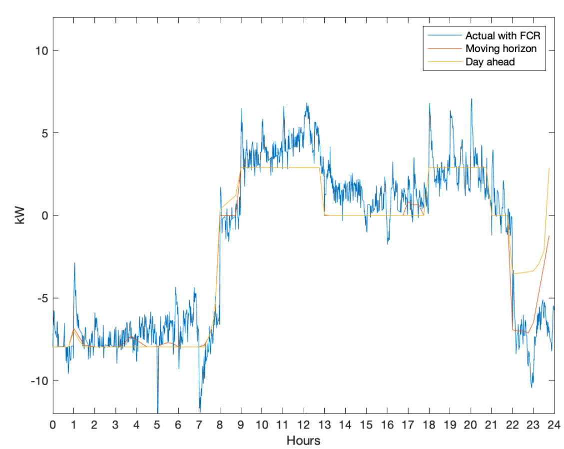

Figure 7.5: Power grid exchange with different schedules of one household

In order to evaluate the effects that FCR integration have on the feeder, the power exchange of all 55 prosumers is presented in figure 7.6. It is important to remark that the input data and constraints are identical to the case with peak tariff presented in figure 5.10, except for the FCR consideration. Comparing these two grid exchanges, it is clear that FCR has a significant effect on them. There are several hours with constant power schedules without considering power regulation, especially when storage is available and demand is comparatively lower, e.g., from 2:00 - 6:00 hrs. As expected, once regulation is considered these constant power exchanges disappear because of the stochastic nature of frequency regulation observed in figure 7.3. Furthermore, the peak capacities are frequently surpassed achieving power levels up to -12 kW (drawing), and almost 10 kW (feeding). These peaks coincide with the maximum frequency deviations, e.g., 5:00, 12:00, and 20:00 hrs.

Running the grid exchange profiles in the test feeder model presented in section 3.4, yields the results in figure 7.7. The figure compares the case with and without FCR. It can be seen that the general pattern is consistent in both cases, but the FCR case adds extra stress to the grid due to the extra power. As a consequence, the gird limits are surpassed considerably for long periods of time, especially the upper limits for feeding back in. It can be argued that if there is increasing scarcity of generation coupled with increasing demand, more congestion towards the upper limits would be expected. Scarcity will push energy prices higher incentivizing feed in from prosumers with smart energy systems, on top of this, frequency will deviate below 50 Hz (due to the shortage) and call for extra feed in regulation power. A solution would be to cap the amount of capacity reserved for FCR with the peak tariff (or any other mechanism), however, the frequency deviations are not known in advance and that would represent a loss of opportunity for prosumers' revenue and grid's aid for balancing. This points to one key conflict between the incentives of imbalances at a transmission level and local congestion at a distribution level.

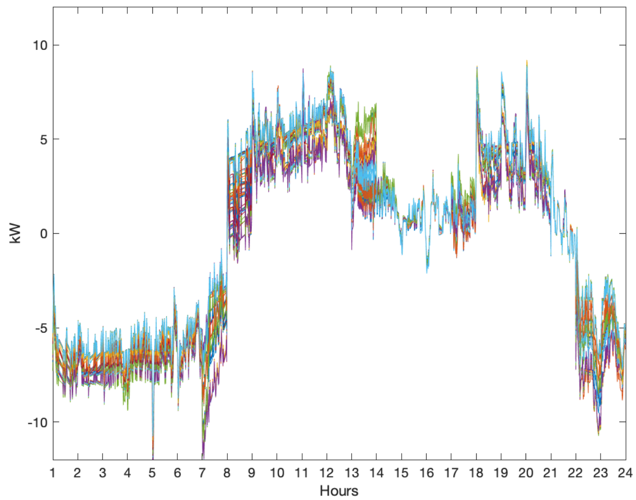

Figure 7.6: Power grid exchange with FCR of all households

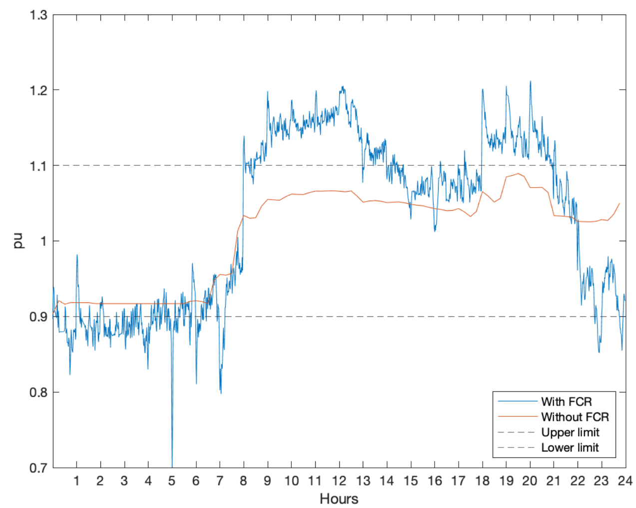

Figure 7.7: Voltage at BUS 906 in the feeder with FCR and without

Lastly, figure 7.8 displays the cost comparison between the incorporation of FCR and not incorporating it to the optimization, for all prosumers in the feeder. The case without FCR does not include the revenue from reserving capacity for regulation making the day ahead costs higher than with FCR. The FCR case has a revenue of 55.84 €, however, it incurs higher costs due to schedule deviations from the day ahead schedule. The effects of these deviations can be seen in the increased costs for intraday trades and imbalance costs. It is relevant to remark that these imbalances are not equal to the power supplied for regulation, they are consequence of the power supplied.

The key issue is that the power called for regulation depends on the frequency deviation, which is not known beforehand, thus, the optimization is updated every time step after providing power for regulation. This causes the deviations from the day ahead schedule, for example, if at an instance close to EV departure a big amount of power (e.g., 5 kW) is called for up regulation from the EV, it will decrease the SoC more than the smart charging algorithm had "accounted for". Then, in the next time step the optimization would compensate by drawing more power than scheduled to satisfy the minimum SoC required from the EV before departure.

This happens due to the fact that the same available storage capacity (EV and BES) is participating in the day ahead and FCR market. To avoid this, capacity would need to be reserved exclusively for FCR, hence, it would not be subject to imbalance penalties due to deviations of schedule. This points towards a trade off between prosumers' flexibility because of the conflicting incentives between markets, discussed above.

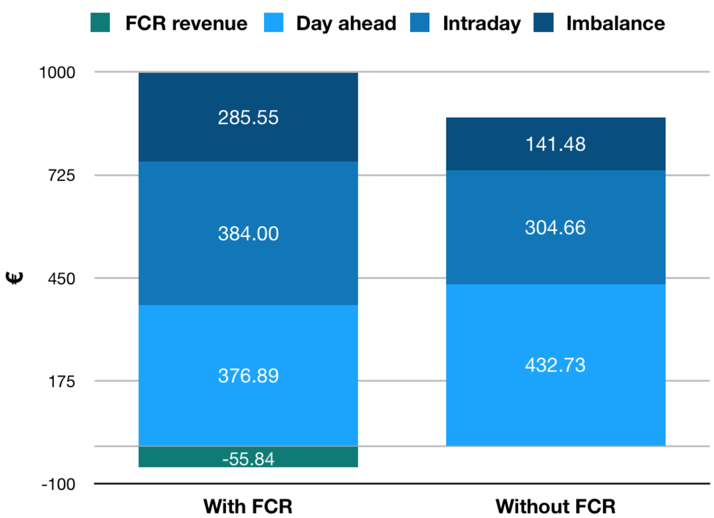

Figure 7.8: Feeder's costs with FCR incorporation and without

8 CONCLUSIONS AND FURTHER RESEARCH

8.1 CONCLUSIONS

The main objective of this thesis was: *to investigate, evaluate and compare the techno-economic feasibility of novel energy market mechanisms that incentivize the involvement of prosumers in demand response and congestion management schemes*. In order to achieve this objective, the formulations, results, and analysis of previous chapters were presented. Figure 8.1 summarizes the key steps taken and insights drawn from this thesis.

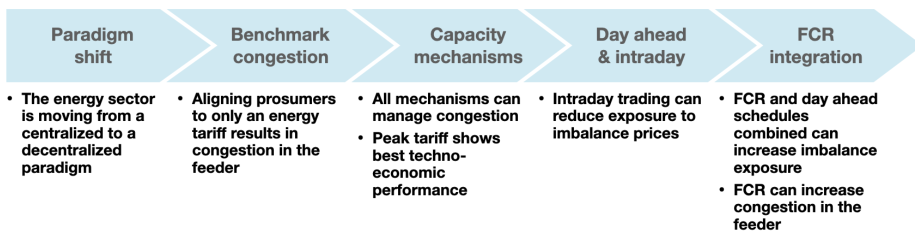

Figure 8.1: Key steps and conclusions

First, the energy sector is facing a shift from a centralized to a decentralized paradigm due to, in part, the penetration of renewable energy sources and increases electrification of the energy sector. This has been part of the effort towards an energy transition away from fossil fuels because of their negative impact on the environment and health. However, this transition comes with serious challenges that are increasingly pressing the energy sector. The challenges that this thesis has focused on have a technical side and economic one. On the technical side, the focus has been on the effects intermittent RES and increased load demand due to electrification have on congestion at a distribution level. For the economic part, the aim has been on the inefficiency that current energy markets have at assigning value to prosumers' demand flexibility. Prosumers are becoming increasingly active players in a decentralized energy sector, therefore, it is key to have properly designed market mechanisms that align them with the economic incentives of the market.

Second, a case study was developed to benchmark congestion in the feeder by aligning prosumers to an energy tariff as the only price signal. This benchmark was achieved by modeling the IEEE European low voltage test feeder with the optimized grid exchange profiles of the 55 households connected in the distribution network. It was assumed that each household would be a prosumer with a PV, EV, and BES connected to a multiport converter where a smart charging algorithm optimizes grid exchange schedules satisfying non flexible load and heating demands, and EV schedules. The development of the smart energy system as an optimization problem was not part of this work, nevertheless, it was adapted to the case study to evaluate congestion levels in two extreme scenarios for winter and summer. The results of this model showed that prosumers can be aligned to the market and allow a more active participation by being demand responsive. Although, if an energy tariff is the only economic signal, then, congestion was present in the feeder in both scenarios. Even though prosumers have individual constraints and requirements, they all have the objective to minimize costs and are incentivized to draw and store at low energy prices to feed in at instances with high prices, whenever possible. Consequently, there are overlaps when the majority of prosumers in the feeder are drawing/feeding near peak power.

Third, a techno economic evaluation of capacity mechanisms for congestion management was conducted. The mechanisms assessed where: 1) hard constraint, 2) capacity subscription, 3) peak tariff, and 4) dynamic tariff. On the technical side, all mechanisms successfully prevented congestion in the feeder in the case study, however, some where more restrictive than others. The hard constraint lost the most amount of load, and the dynamic tariff the least. On the economic side, cost of the lost load was again highest for the hard constraint but lowest for the peak tariff. This may be explained because the dynamic tariff is set to restrict peak capacities at instances when highest demand is expected, whereas the peak tariff sets a price for the whole time period (one day in this case) regardless of the instance when the peak is achieved. Finally, the total cost incurred by all prosumers in the feeder was highest for the capacity subscription because the subscription level is not a decision variable but a parameter (unlike the peak and dynamic tariff) and it is allowed to be surpassed at a high penalty; the hard constraint physically limits the load above the subscription level, hence, no penalty is paid. The peak tariff incurred the lowest overall cost to the whole feeder, thus, it was selected as the best performing mechanism to build on top of it the next markets.

Fourth, the day ahead and intraday market were incorporated to the peak tariff in order to minimize the exposure to imbalance costs due to forecast error, previously not considered. The smart charging algorithm relies on forecasted data to output optimized power exchange schedules, however, these forecasts are not 100% accurate and will cause deviations between the actual and scheduled power exchange, these deviations are subject to imbalance costs. The incorporation of the day ahead and intraday market works by setting an optimized power schedule (and peak capacity) before day ahead closure (11:45 hrs) with the best available forecast at that instance. Then, as time passed the optimization in the moving horizon corrects deviations based on new more accurate forecasts by trading intradaily one time step before delivery (t-15min). By adding this incorporation to the optimization, the imbalance costs were indeed reduced for prosumers in the feeder, furthermore, it aligns the whole model closer to the real situation in current markets.

Last, it was assessed wether it is feasible to additionally include the participation in the frequency containment reserve market. The development of this market in the smart charging algorithm was not part of this work, but it was adapted to all prosumers in the feeder. The assessment was centered around the implications that FCR have on power schedules of prosumers, and the effects on congestion in the feeder. It showed that it is possible to include FCR with the other markets studied, however, it significantly increased the peak capacity achieved by prosumers. Additionally, it may increase imbalance costs because the power provided for regulation requires extra compensation in subsequent time steps to satisfy inner constraints, thus, deviating from day ahead schedules. Moreover, the surpassing of peak capacities achieved resulted in increased congestion in the feeder. These results point to conflicting incentives between balancing and local congestion.

8.2 FURTHER RESEARCH

Once the main results and conclusions have been discussed, the following are some recommendations for further research related to the implementation of market mechanisms for demand response in future decentralized energy systems.

- To simulate different scenarios with longer time horizons in order to have more representative results. Consider a broader range of EV and BES capacities for prosumers in the feeder.
- To investigate and determine which players in the energy sector will take the different roles needed, while maintaining transparency and no conflict of interests. For example, what role do retail companies will have?; who will be the aggregator intermediary between prosumers and the market and how will potential gaming be avoided?; if prosumers become more active participants in the market, will they bear the same participation in financial risk due to price volatility?
- To develop proper schemes that can resolve the conflicting incentives between different markets and levels of operation. For example, the conflicting interests between balancing the grid at a TSO level and managing congestion at a DSO level.

BIBLIOGRAPHY

Amstel, M. v. (2018). *Flexibility system design for electric vehicles. Performing congestion management for the DSO*. PhD thesis.

Bhagwat, P. C., Iychettira, K. K., Richstein, J. C., Chappin, E. J., and De Vries, L. J. (2017). The effectiveness of capacity markets in the presence of a high portfolio share of renewable energy sources. *Utilities Policy*, 48:76–91.

Bjarghov, S. and Doorman, G. (2018). Utilizing end-user flexibility for demand management under capacity subscription tariffs. *International Conference on the European Energy Market, EEM*, 2018-June.

B.V, A. P. X. H. (2018). EPEX Spot Dashboard market results.

Chandra Mouli, G. R., Schijffelen, J. H., Bauer, P., and Zeman, M. (2017). Design and Comparison of a 10-kW Interleaved Boost Converter for PV Application Using Si and SiC Devices. *IEEE Journal of Emerging and Selected Topics in Power Electronics*, 5(2):610–623.

Council of European Energy Regulators (2009). European Regulators' Group for Electricity and Gas Contact. Technical report.

de Vries, L. and Doorman, G. (2021). *Valuing consumer flexibility in electricity market design*. Elsevier Inc.

Doorman, G. and De Vries, L. (2017). Electricity market design based on consumer demand for capacity. *Eurelectric-Florence School of Regulation Conference*.

Dudgeon, G. (2021). Distribution System Model in Simscape : European Test Feeder, MATLAB Central File Exchange.

Ellabban, O., Abu-Rub, H., and Blaabjerg, F. (2014). Renewable energy resources: Current status, future prospects and their enabling technology.

Enerdata (2020). World Energy Statistics. Technical report.

EPEX SPOT (2021). Trading at EPEX SPOT 2021. Technical report.

ev-database.org (2021). Tesla Model 3 Standard Range.

Fonteijn, R., Amstel, M., Nguyen, P., Morren, J., Maarten Bonnema, G., and Slootweg, H. (2019). Evaluating flexibility values for congestion management in distribution networks within Dutch pilots. *The Journal of Engineering*, 2019(18):5158–5162.

Fouquet, R. (2016). Historical energy transitions: Speed, prices and system transformation. *Energy Research and Social Science*, 22:7–12.

Frontier Economics (2015). Scenarios for the Dutch electricity supply system. Technical Report September.

Green, M. A. (2016). Commercial progress and challenges for photovoltaics.

GSMArena. Apple iPhone 12 Pro Max - Full phone specifications.

GSMArena. Nokia 3310 - Full phone specifications.

Haque, A. N., Nguyen, P. H., Kling, W. L., and Bliek, F. W. (2014). Congestion management in smart distribution network. *Proceedings of the Universities Power Engineering Conference*, (Mv).

Haque, A. N., Shafiullah, D. S., Nguyen, P. H., and Bliek, F. W. (2016). Real-time congestion management in active distribution network based on dynamic thermal overloading cost. *19th Power Systems Computation Conference, PSCC 2016*.

Haque, A. N., Vo, T. H., Nguyen, P. H., Slootweg, J. G., and Bliek, F. W. (2018). Smart real-time multi-node congestion management in active distribution networks. *IEEE Power and Energy Society General Meeting*, 2018-Janua:1–5.

IEA (2020a). Global EV Outlook 2020 – Analysis. Technical report.

IEA (2020b). Heating – Analysis. Technical report.

IEA (2020c). World Energy Outlook 2020 – Analysis. Technical report.

IEEE (2015). 2015 Test Feeder Cases.

J. de Vries, F. Correljé, P.A. Knops, and Reinier van der Veen (2019). Electricity Markets SET3055.

Jin, X., Wu, Q., and Jia, H. (2020). Local flexibility markets: Literature review on concepts, models and clearing methods. *Applied Energy*, 261.

Klein, M., Ziade, A., and de Vries, L. (2019). Aligning prosumers with the electricity wholesale market – The impact of time-varying price signals and fixed network charges on solar self-consumption. *Energy Policy*, 134.

Koliou, E., Bartusch, C., Picciariello, A., Eklund, T., Söder, L., and Hakvoort, R. A. (2015). Quantifying distribution-system operators' economic incentives to promote residential demand response. *Utilities Policy*, 35:28–40.

Lang, T., Ammann, D., and Girod, B. (2016). Profitability in absence of subsidies: A techno-economic analysis of rooftop photovoltaic self-consumption in residential and commercial buildings. *Renewable Energy*, 87:77–87.

Martinot, E. (2016). Grid Integration of Renewable Energy: Flexibility, Innovation, and Experience. *Annual Review of Environment and Resources*, 41:223–251.

MIT Energy Initiative (2016). *UTILITY OF THE FUTURE An MIT Energy Initiative response*.

Moriarty, P. and Honnery, D. (2016). Can renewable energy power the future? *Energy Policy*, 93:3–7.

Mouli, G. R. C., Bauer, P., and Zeman, M. (2016). System design for a solar powered electric vehicle charging station for workplaces. *Applied Energy*, 168:434–443.

NREL (2015). Battery value versus remaining energy.

Ottesen, S. , Tomasgard, A., and Fleten, S. E. (2018). Multi market bidding strategies for demand side flexibility aggregators in electricity markets. *Energy*, 149:120–134.

Philipsen, R., Morales-España, G., de Weerdt, M., and de Vries, L. (2019). Trading power instead of energy in day-ahead electricity markets. *Applied Energy*, 233-234(January 2018):802–815.

Piao, L., De Vries, L., De Weerdt, M., and Yorke-Smith, N. (2019). Electricity markets for DC distribution systems: Design options. *Energies*, 12(14):1–16.

Piao, L., de Vries, L., de Weerdt, M., and Yorke-Smith, N. (2021). Electricity markets for DC distribution systems: Locational pricing trumps wholesale pricing. *Energy*, 214:118876.

Pillay, A., Prabhakar Karthikeyan, S., and Kothari, D. P. (2015). Congestion management in power systems - A review. *International Journal of Electrical Power and Energy Systems*, 70:83–90.

SEDC (2016). Explicit and Implicit Demand-Side Flexibility. *Position Paper*, (September).

Singh, A., Reese, S., and Akar, S. (2019). Performance and Techno-Economic Evaluation of a Three-Phase, 50-kW SiC-Based PV Inverter. In *2019 IEEE 46th Photovoltaic Specialists Conference (PVSC)*, pages 695–701.

Stawska, A., Romero, N., de Weerdt, M., and Verzijlbergh, R. (2021). Demand response: For congestion management or for grid balancing? *Energy Policy*, 148(PA):111920.

Stoll, C., Klaaßen, L., and Gallersdörfer, U. (2019). The Carbon Footprint of Bitcoin. *Joule*, 3(7):1647–1661.

Tennet (2015). The Imbalance Pricing System.

TenneT (2018a). End report FCR pilot. Technical report.

TenneT (2018b). Product information aFRR (Regulating power).

TenneT (2019). Annual Market Update 2019. Technical report.

Tennet (2019). Product information on reactive power.

TenneT (2020). Imbalance Pricing System. Technical report.

TenneT (2021a). Ancillary Services.

TenneT (2021b). FCR Manual for BSP's. Technical report.

van Melle, T., Menkveld, M., Oude Lohuis, J., de Smidt, R., and Terlouw, W. (2015). De systeemkosten van warmte voor woningen. Technical report, Ecofys Netherlands B.V.

Veldman, E. (2013). *Power Play Impacts of flexibility in future residential electricity demand on distribution network utilisation*. PhD thesis, Technische Universiteit Eindhoven.

Vermeer, W., Mouli, G. R. C., and Bauer, P. (2020). Real-time building smart charging system based on PV forecast and Li-Ion battery degradation. *Energies*, 13(13):1–23.

Wang, J., Purewal, J., Liu, P., Hicks-Garner, J., Soukazian, S., Sherman, E., Sorenson, A., Vu, L., Tataria, H., and Verbrugge, M. W. (2014). Degradation of lithium ion batteries employing graphite negatives and nickel–cobalt–manganese oxide + spinel manganese oxide positives: Part 1, aging mechanisms and life estimation. *Journal of Power Sources*, 269:937–948.

A APPENDIX

.1 NON LINEAR PROGRAMMING MODEL

This model was developed by [56], and adapted for this thesis as presented in chapter 3. This sections elaborates on the constraints and limitations of the optimization problem.

.1.1 Objective function

$$min(C_{Total}) = min(C_{BES} + C_{EV} + C_{PV} + C_{Grid} - C_{Reg}) \tag{.1}$$

Battery costs

$$V_{BES} = \frac{V_{BES}^{2nd} - V_{BES}^{new}}{0.2} \Delta E_{BES}^{Total} + V_{BES}^{new} \tag{.2}$$

$$C_{BES} = V_{BES}^{new} E_{BES}^{max} - V_{BES}(E_{BES}^{max} - \Delta E_{BES}^{Total}) \tag{.3}$$

Electric vehicle costs

$$V_{EV} = \frac{V_{EV}^{2nd} - V_{EV}^{new}}{0.2} \Delta E_{EV}^{Total} + V_{EV}^{new} \tag{.4}$$

$$C_{EV} = V_{EV}^{new} E_{EV}^{max} - V_{EV}(E_{EV}^{max} - \Delta E_{EV}^{Total}) \tag{.5}$$

Photovoltaic costs

$$C_{PV} = \sum_{t=1}^{T} P_{PV}(t) \Delta t \lambda_{PV} \quad \forall t \tag{.6}$$

Grid costs

$$C_{Grid} = \sum_{t=1}^{T} P_{Grid}^{Buy}(t) \lambda_{Buy}(t) \Delta t - \sum_{t=1}^{T} P_{Grid}^{Sell}(t) \lambda_{Sell}(t) \Delta t \quad \forall t \tag{.7}$$

Regulation revenue

$$C_{Reg} = \eta_{inv} \eta_{ch} \sum_{t=1}^{T} (P_{Reg}^{Up}(t) \lambda_{Up}(t) + P_{Reg}^{Down}(t) \lambda_{Down}(t)) \Delta t \quad \forall t \tag{.8}$$

.1.2 Constraints and limitations

Power balance and limitations

$P_{inv}(t)$ is the power balance on the DC link of the multiport converter, connecting PV power $P_{PV}(t)$, BES power $P_{BES}(t)$, and EV power $P_{EV}(t)$. $P_{grid}(t)$ is the power balance of the AC side, between the inverter and the meter. $P_{appl.}(t)$ and $P_{heat}(t)$ are non-flexible appliances and heating loads, respectively. $P_X(t)$ are the bidirectional power flows of BES, EV, and inverter, where there is a distinction between positive (charge), and negative (discharge) powers. η_X are the efficiencies: 96% for BES and EV, and 98% for the inverter.

$$P_{inv}(t) = P_{PV}(t) - P_{BES}(t) - P_{EV}(t) \quad \forall t \tag{.9}$$

$$P_{grid}(t) = P_{inv}(t) - P_{appl.}(t) - P_{heat}(t) \qquad \forall t \tag{.10}$$

$$P_X(t) = \eta_X P_X^+(t) - \frac{1}{\eta_X} P_X^-(t) \qquad \forall t \tag{.11}$$

Grid constraints

The grid power for feeding $P^+_{grid}(t)$ and drawing $P^-_{grid}(t)$ is constrained by the the physical connection $P^{max}_{grid} = 17.5$ kW. Additionally, $\eta_{cable} = 98\%$ is introduced as a soft constraint to avoid the use of binary variables by making the optimization recognize losses and not allowing non-zero feed/draw power simultaneously.

$$P^-_{grid}(t) \leq P^{max}_{grid} \qquad \forall t \tag{.12}$$

$$P^+_{grid}(t) \leq P^{max}_{grid} \qquad \forall t \tag{.13}$$

$$P_{grid}(t) = \eta_{cable} P^+_{grid}(t) - \frac{1}{\eta_{cable}} P^-_{grid}(t) \qquad \forall t \tag{.14}$$

Energy balance and limitations

For this model it is assumed that N^{series}_{cell} and $N^{parallel}_{cell}$ single Li-ion cells form the energy storage pack of the BES and EV, E^{rated}_X. Once the model has started ($t > 0$), the storage capacity $E^{max}_X(t)$ decreases by $\Delta E_X(t)$ according to the degradation model (presented below), thus, the energy charge of the BES and EV $E_X(t)$ at any instance are limited. The SoC is managed between 10% and 90%. Additionally, $\gamma(t)$ is a parameter introduced to denote the availability of the EV (figure 4.7) and make $P_{EV}(t) = 0$ when not available, it is assumed a reduction of energy due to EV's commute $P_{drive}(t)$, and E^{depart}_{EV} is the minimum EV charged required by the user before leaving at t_{depart}.

$$E^{rated}_X = \frac{N^{series}_{cell} N^{parallel}_{cell}}{1000} V^{nom}_{cell} Q_{cell,nom} \tag{.15}$$

$$E^{max}_X(t) = \begin{cases} E^{rated}_X, & \text{for } t = 1 \\ E^{max}_X(t-1) - \Delta E_X(t), & \text{for } t > 1 \end{cases} \tag{.16}$$

$$E_X(t) \leq E_X^{max}(t) \qquad \forall t \tag{.17}$$

$$SoC_X(t) = \frac{E_X(t)}{E_X^{max}(t)} \qquad \forall t \tag{.18}$$

$$0.1 \leq SoC_X(t) \leq 0.9 \qquad \forall t \tag{.19}$$

$$E_{BES}(t) = E_{BES}(t-1) + P_{BES}(t)\Delta t \qquad \text{for } t > 1 \tag{.20}$$

$$E_{EV}(t) = E_{EV}(t-1) + (\gamma(t)P_{EV}(t) - P_{drive}(t))\Delta t \qquad \text{for } t > 1 \tag{.21}$$

$$E_{EV}(t) = E_{EV}^{depart} \qquad \text{for } t > t_{depart} \tag{.22}$$

EV and BES constraints

EV and BES power ($P_X(t)$) are limited by their maximum power $P_X^{max}(t)$ which depends on the SoC. Here, three different regions for (dis)charge are recognized: 1) pre-charge region (very low SoC), 2) constant charge, and 3) constant voltage region; thus $D_{ch/dis}$ sets the limit for constant charge region, [56] for further reference. Lastly, the maximum power $P_X^{max}(t)$ is limited by the power rating P_X^{Rated} which depends on the C-rate and size of the battery. The C-rate for the EV and BES considered is equal to 1.

$$P_X^{+}(t) \leq P_X^{max}(t) \qquad \forall t \tag{.23}$$

$$P_X^{max}(t) \leq P_X^{rated} \qquad \forall t \tag{.24}$$

$$P_X^{max}(t) \leq \frac{P_X^{rated}}{(1-D_{ch})}\left(\frac{E_X(t)}{E_X^{max}} - 1\right) \qquad \forall t \tag{.25}$$

$$P_X^{-}(t) \leq P_X^{min}(t) \qquad \forall t \tag{.26}$$

$$P_X^{min}(t) \leq P_X^{rated} \qquad \forall t \tag{.27}$$

$$P_X^{min}(t) \leq \frac{P_X^{rated}}{D_{dis}}\frac{E_X(t)}{E_X^{max}} \qquad \forall t \tag{.28}$$

Energy storage degradation model

The cost of energy storage degradation is modeled for the BES and EV based on a single Nickel-Manganese-Cobalt (NMC) cell. A distinction is made between lost capacity due to cyclic and calendar aging, $\Delta E_X^{cycle}(t)$ and $\Delta E_X^{cal}(t)$ respectively. $V_{oc}^{linear}(t)$ is the linerized open circuit voltage of an NMC cell, and $\Delta E_X^{cal}(t)$ is linerized with a fixed percentage per time step.

$$V_{oc}^{linear}(t) = N_{cell}^{series}(i)\Big(3.42 + 0.7SoC_X(t)\Big) \qquad \forall t \tag{.29}$$

$$i_X^{cell}(t) = \frac{P_X(t)}{N_{cell}^{parallel} V_{oc}^{linear}(t)} \qquad \forall t \tag{.30}$$

$$\Delta E_X^{\%}(t) = c_1 e^{c_2 |I_X^{cell}(t)|} i_X^{cell}(t) |I_X^{cell}(t)| \Delta t \qquad \forall t \tag{.31}$$

$$\Delta E_X^{cycle}(t) = \Big(\Delta E_X^{\%}(t)\Big)\frac{E_X^{rated}}{100} \quad , \forall t \tag{.32}$$

$$\Delta E_X^{cal}(t) = \Big(c_3\sqrt{t}e^{-24kJ/RT}\Big)\frac{E_X^{rated}}{100} = \Big(c_4 \Delta t\Big)\frac{E_X^{rated}}{100} \qquad \forall t$$

$$\Delta E_X^{tot} = \sum_{t=0}^{T}\Big(\Delta E_X^{cycle}(t) + \Delta E_X^{cal}(t)\Big) \quad \forall t \tag{.33}$$

TU Delft